Supplement of Hydrol. Earth Syst. Sci., 26, 1131–1143, 2022
https://doi.org/10.5194/hess-26-1131-2022-supplement

Hydrology and Earth System Sciences
Open Access

Supplement of

Temporally resolved coastal hypoxia forecasting and uncertainty assessment via Bayesian mechanistic modeling

Alexey Katin et al.

Correspondence to: Alexey Katin (akatin@ncsu.edu)

Supporting information

Contents

S1 DMO20 model description

DMO20 model, fully described in Del Giudice et al. (2020), is based on a steady-state solution to mass balance differential equations presented in Obenour et al. (2015). Using time-varying inputs, DMO20 predicts daily BWDO (O_b) concentration (mg/L) from 1 June to 30 September of each year:

$$O_b = \frac{(k_a O_s - D_w)}{k_a - D_s/O_f} - 1 \quad \text{(S1.1)}$$

where k_a is the reaeration rate (m/d), D_w is the water column oxygen demand (WCOD), and D_s is the sediment oxygen demand (SOD) at O_f, a reference oxygen concentration set to 3 mg/L.

The net WCOD (g/m^2/d) of each lower compartment is represented as:

$$D_w = J\gamma\omega = \left(\lambda \frac{L_r + L_u}{(Q_r + Q_u + Q_g)/\nu + A}\right)\gamma\omega. \quad \text{(S1.2)}$$

Here, J is the downward carbon flux (g/m^2/d), γ is the mass ratio of oxygen demand to organic carbon set to 3.5, λ is the ratio of organic carbon to nitrogen set to 5.68, A is the area of the shelf section (Gm^2), ω is an oxygen demand adjustment factor (accounting for photosynthesis, off-shelf losses, etc.), and ν is the effective settling velocity (m/d), which incorporates both the production and sinking of organic matter. The variables Q and L represent the near-term flows (Gm^3/d) and N loads (Gg/d) entering the surface-layer model compartments, respectively. Subscripts r, u, and g denote the origin of these fluxes: Mississippi and Atchafalaya Rivers, upstream (i.e., eastern) shelf section, and the greater Gulf of Mexico. Q_g is approximated as a dilution factor (3.2, derived from surface salinity data) multiplied by mean Mississippi River discharge (1.6 Gm^3/d).

The reaeration rate for each section is determined as a function of wind stress (representing shear-induced turbulence) and freshwater flow (representing buoyancy):

$$k_a = \beta_0 + \beta_1 \frac{U^2}{Q_s} \frac{A}{10000} \quad \text{(S1.3)}$$

where U is the 14-day weighted mean wind speed for the shelf section (m/s), Q_s is the river discharge entering the section (Gm^3/d), and β_0 and β_1 are calibration parameters.

Partitioning of riverine inputs is computed through:

$$F_W = 0.5 - \beta_e v_e \quad \text{(S1.4)}$$

where F_W is the fraction of abovementioned flows and loads transported westward over the shelf, v_e is the mean eastward wind velocity (m/s), and β_e is a calibration parameter. The 0.5 indicates that, in absence of wind, inputs from both rivers would equally partition westward and eastward.

SOD is represented as:

$$D_s = B\sqrt{\frac{L}{\bar{L}}}\theta^{T-\bar{T}}. \quad \text{(S1.5)}$$

where L (Mg/mo) is the combined nutrient loading from the Mississippi and Atchafalaya Rivers, averaged November-March. We normalize these pre-spring loads relative to their long-term average ($\bar{L}$) for the study period. SOD is temperature dependent and is based on the Arrhenius model with $\theta = 1.07$. Rates are corrected when temperatures deviate from $\bar{T}$, the summertime average. Here, T is the monthly mean temperature.

A quadratic polynomial function g is used to transform modelled bottom water dissolved oxygen (mg/L) into hypoxic area (km^2). For each section of the shelf, west and east, g is:

$$HA_{West} = g(BWDO_{West}) = 62628 - 21353 \times BWDO_{West} + 1839 \times BWDO_{West}^2 \quad \text{(S1.6)}$$

$$HA_{East} = g(BWDO_{East}) = 17436 - 5945 \times BWDO_{East} + 507 \times BWDO_{East}^2 \quad \text{(S1.7)}$$

For Eq. S6 the $R^2 = 0.98$ and the residual standard deviation is 706 km^2, while for Eq. S7 the $R^2 = 0.99$ and the residual standard deviation is 216 km^2.

Table S1: Summary of the DMO20 model parameters estimated through Bayesian inference, including mean and 95% credible interval of each parameter.

Parameter	Units	Description	2.5%	Mean	97.5%
ν	m/d	effective settling velocity	0.105	0.218	0.360
ω	—	oxygen demand adjustment factor	0.074	0.184	0.368
β_0	m/d	reaeration parameter	0.108	0.168	0.246
β_1	—	reaeration parameter	0.228	0.342	0.468
B	g/m^2/d	average sediment respiration rate	0.225	0.335	0.446
β_e	s/m	east-west advection coefficient	0.152	0.177	0.197
$\sigma_{m,w}$	mg/L	model error, west	0.289	0.375	0.460
$\sigma_{m,e}$	mg/L	model error, east	0.274	0.342	0.421

S2 Bias adjustment for model predictions in June

Preliminary analysis indicated that hindcasted BWDO was somewhat lower than observations for the west section of the shelf in June. This bias remained after conversion of BWDO to HA. A linear regression with zero intercept and a sequence of numbers 29 to 0 representing period from June 1 to June 30 as the predictor was used to estimate a bias adjustment, defined as difference between average observed and hindcasted BWDO divided by hindcasted BWDO. The resulting regression indicates a gradual decline in bias from the beginning of June (Fig. S2.1). The bias adjustment increases the R^2 of relationship between observed and hindcasted BWDO from –0.15 to 0.36 (Fig. S2.2), and between observed and hindcasted HA from –0.14 to 0.45 (Fig. S2.3).

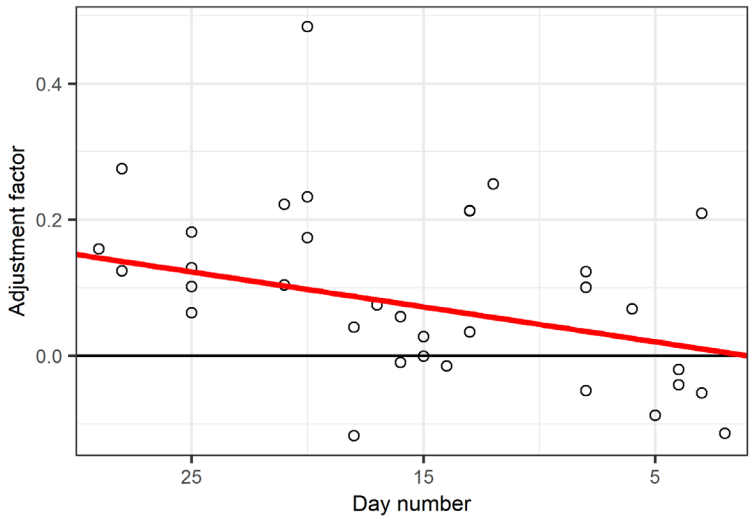

Figure S2.1: Bias adjustment factor vs day number (before 1 July) for the west section with red line showing the regression fit with slope mean and standard error of 0.007 and 0.001, respectively. The adjusted R^2 of this regression is 0.20.

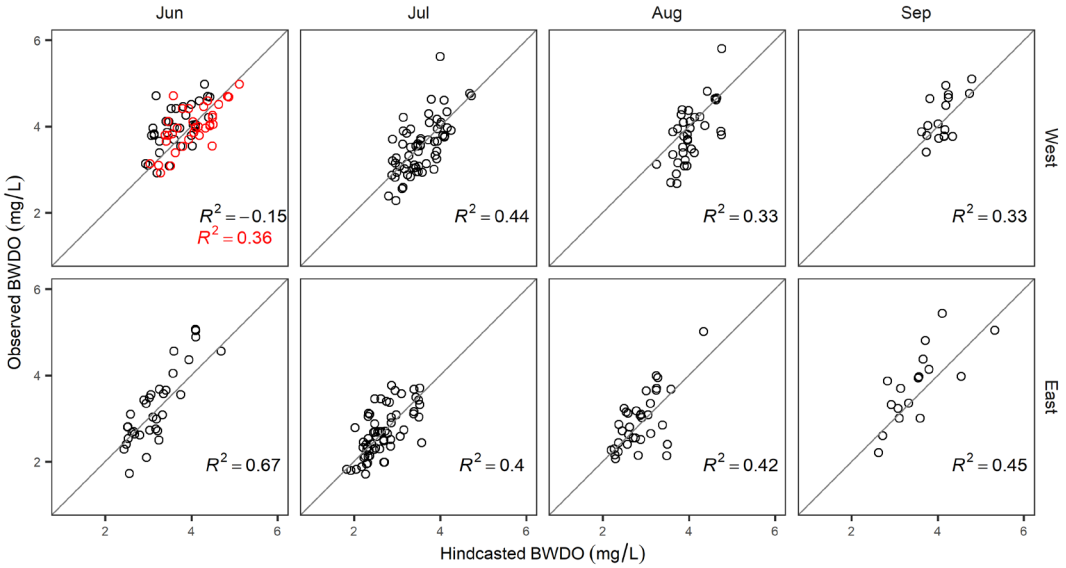

Figure S2.2: Month by month comparison of observed with hindcasted (black) and bias-adjusted hindcasted (red) averaged BWDO in the west and east sections. Diagonal lines represent perfect prediction.

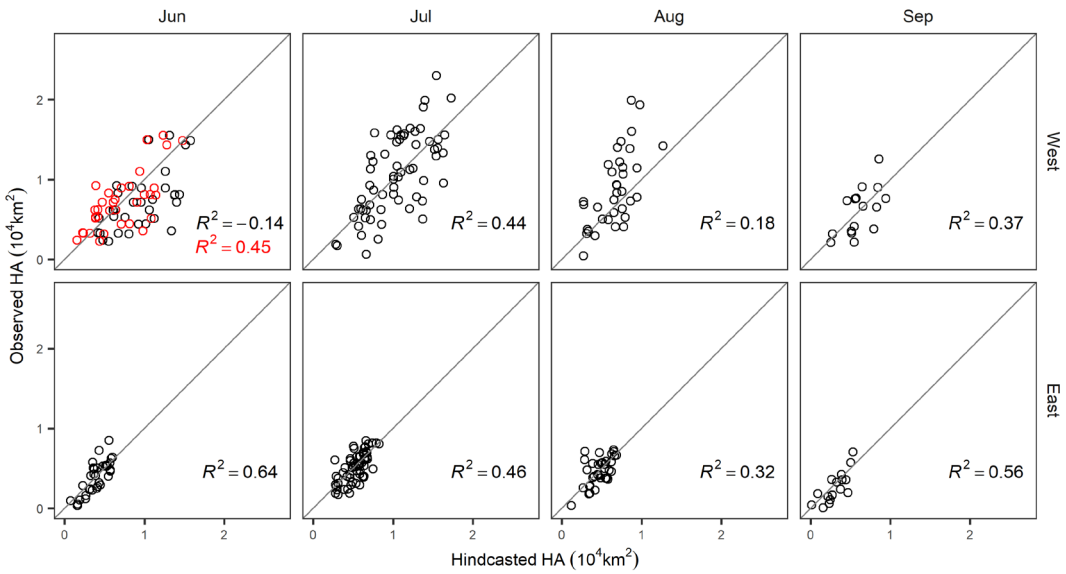

Figure S2.3: Month by month comparison of observed with hindcasted (black) and bias-adjusted hindcasted (red) averaged HA in the west and east sections. Diagonal lines represent perfect prediction.

S3 Regressions for predicting summer Mississippi and Atchafalaya River flow and loading

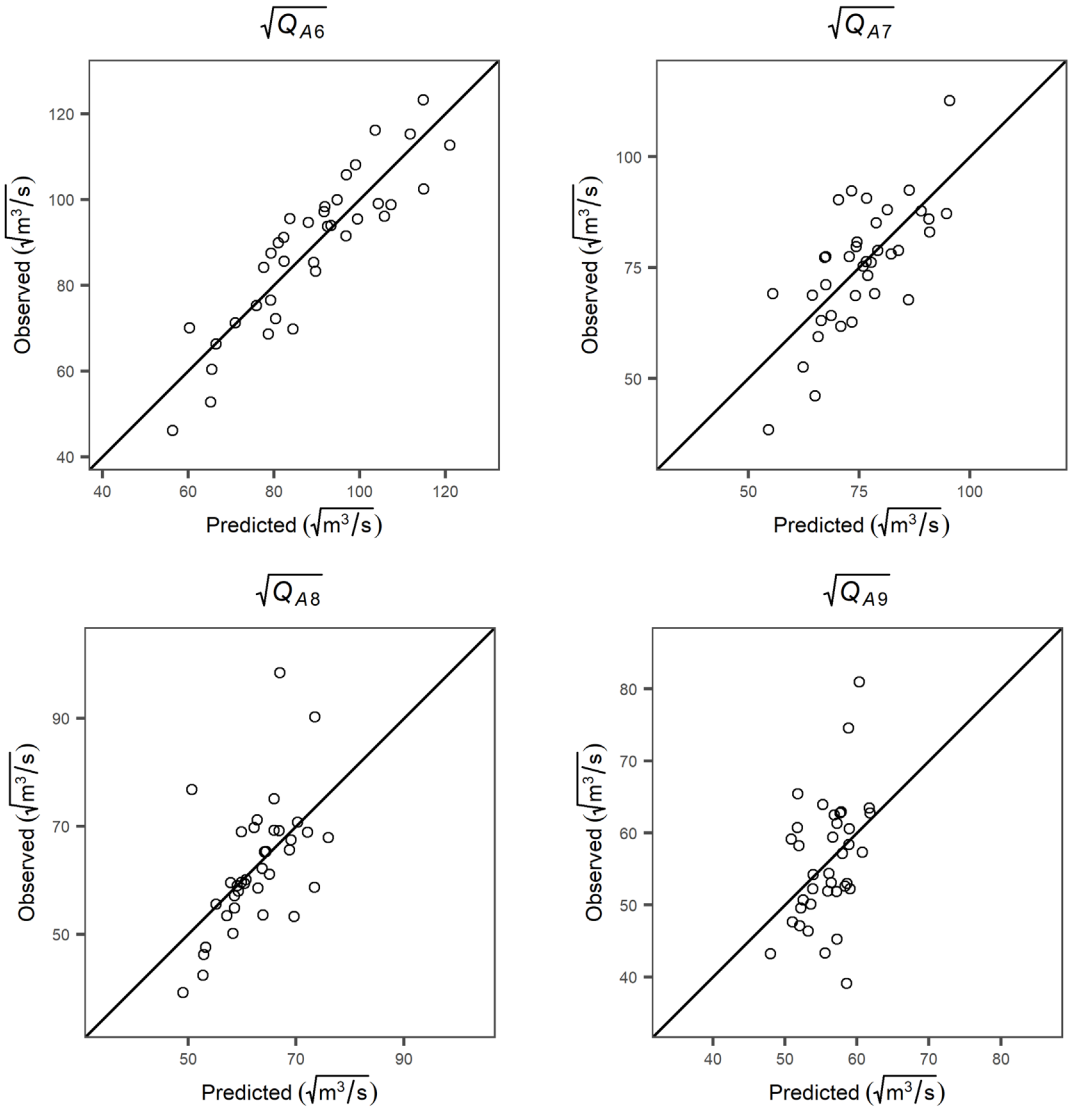

Figure S3.2: Observed versus predicted by regressions square-root transformed Atchafalaya River monthly average discharge. Subscript numbers indicate months (June-September).

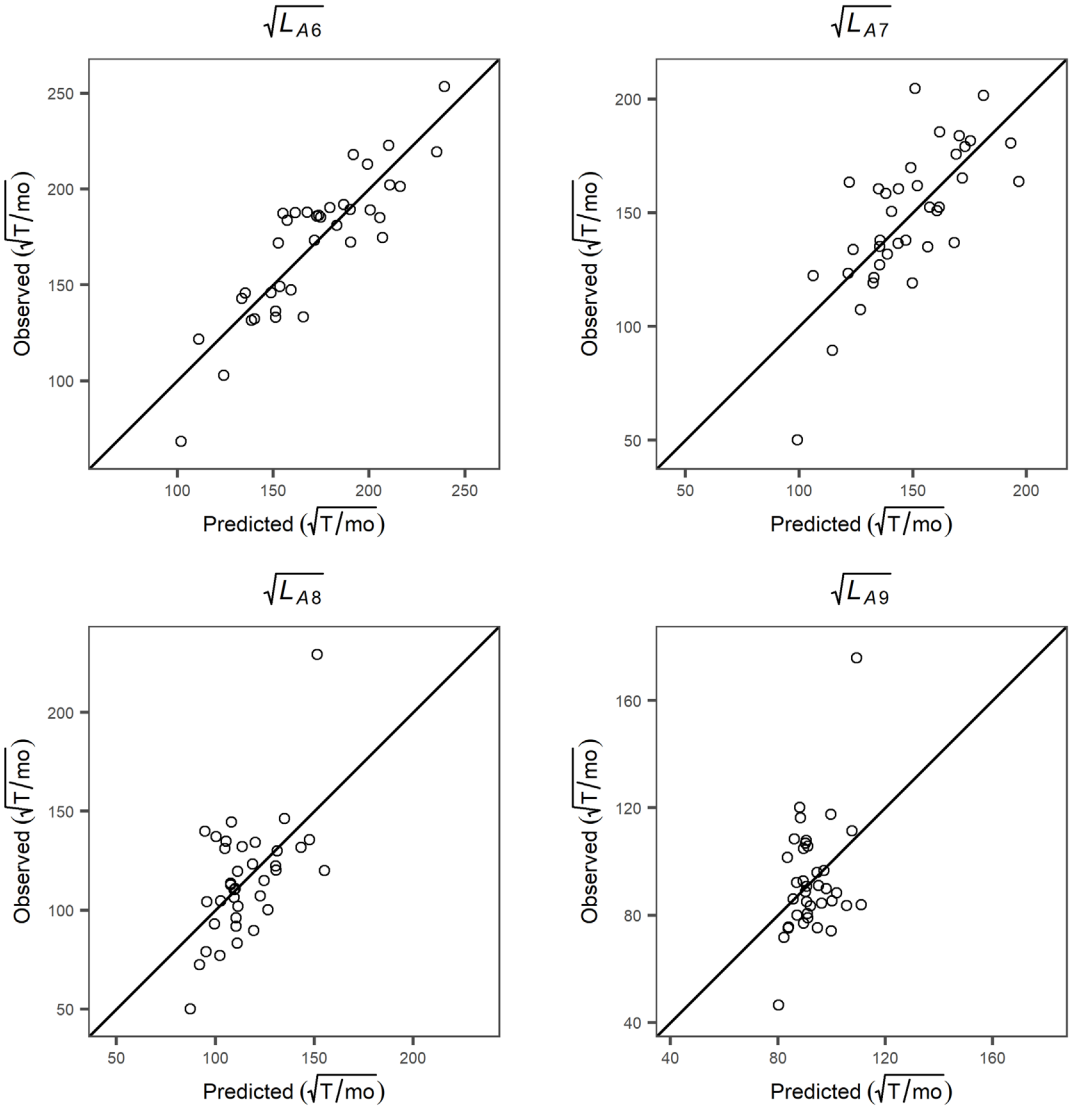

Figure S3.3: Observed versus predicted by regressions square-root transformed Atchafalaya River monthly average nitrogen loading. Subscript numbers indicate months (June-September).

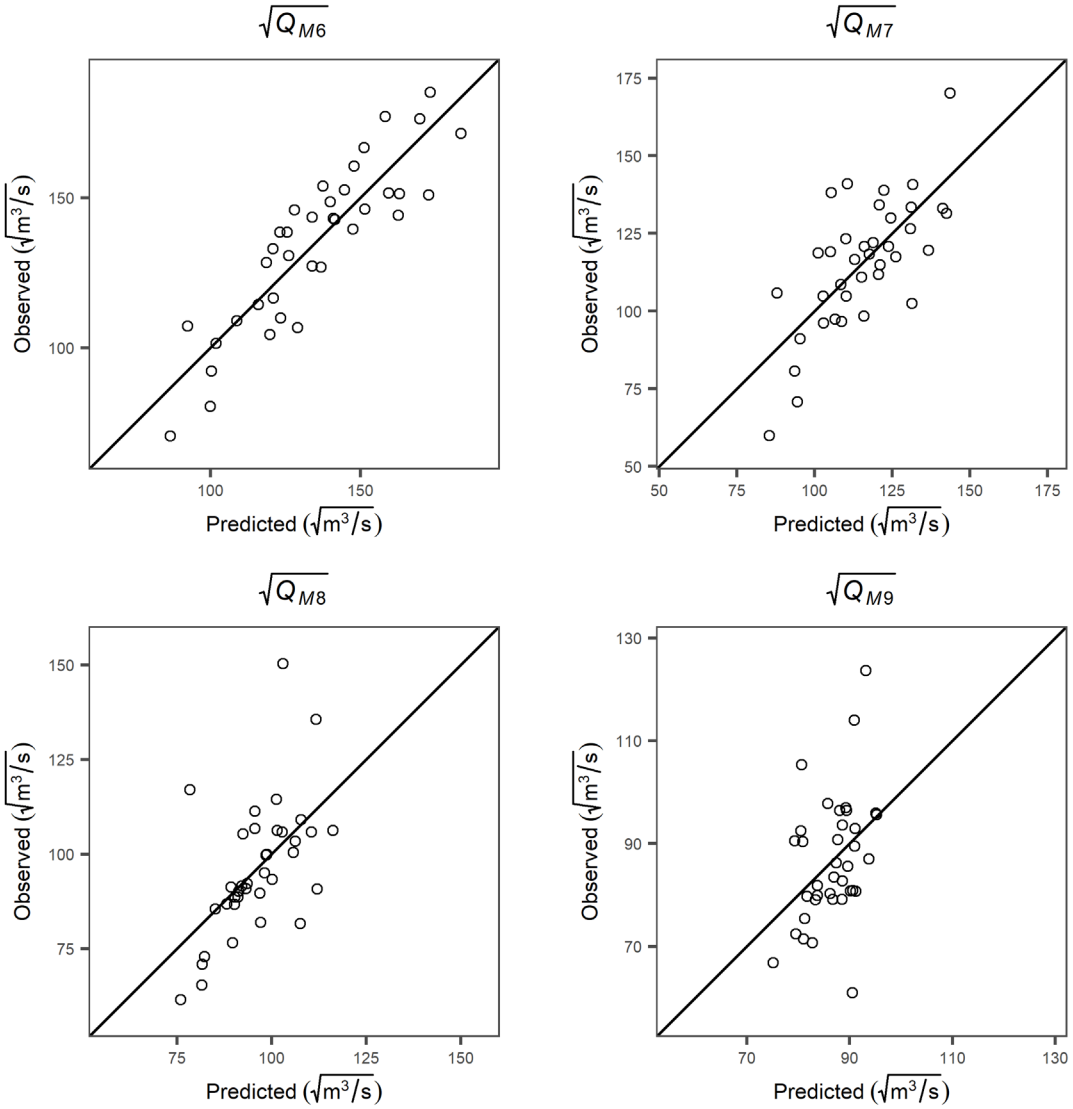

Figure S3.4: Observed versus predicted by regressions square-root transformed Mississippi River monthly average discharge. Subscript numbers indicate months (June-September).

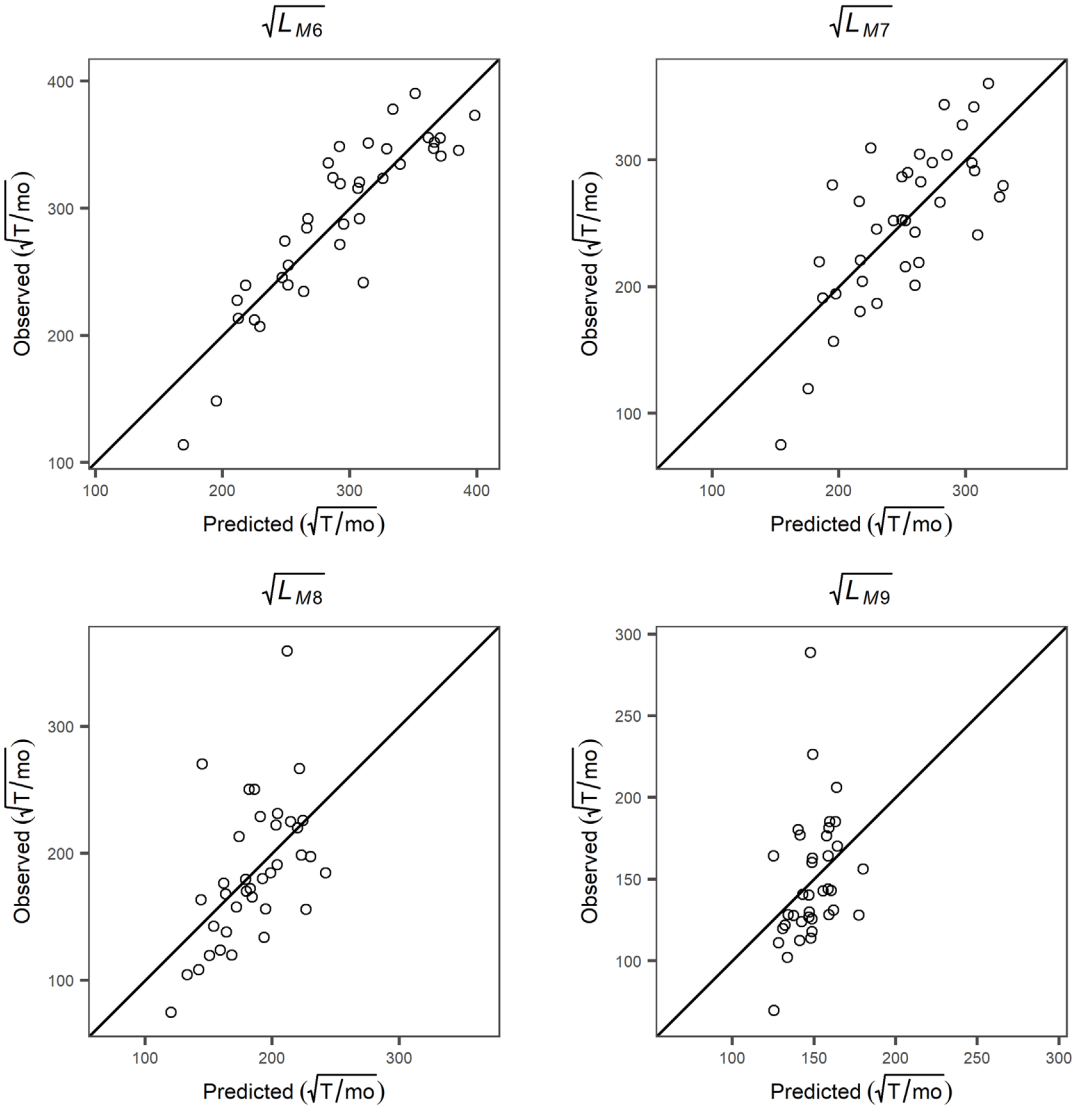

Figure S3.5: Observed versus predicted by regressions square-root transformed Mississippi River monthly average nitrogen loading. Subscript numbers indicate months (June-September).

Table S3.1: Predicted by the regressions (pre) and observed (obs) monthly Atchafalaya River discharge and nitrogen loading

Year	Atchafalaya River															
	Discharge (m^3/s)								Loading (t/mo)							
	Jun		Jul		Aug		Sep		Jun		Jul		Aug		Sep	
	pre	obs	pre	obs	pre	obs	pre	obs	pre	obs	pre	obs	pre	obs	pre	obs
1980	6267	5860	4719	4130	3429	3270	3466	3410	23542	22304	18328	16168	11974	12183	8138	11426
1981	7743	8970	5517	6360	3872	4870	2699	3390	28095	35351	20638	25812	10072	18866	7413	11767
1982	8692	8820	7035	6220	4148	4270	3805	4030	32188	36213	23060	26246	10964	17236	7757	14451
1983	13167	15200	6754	6100	5385	3450	3088	1880	57267	64260	38645	26815	24069	14452	12311	7060
1984	8963	9990	5293	6010	4229	3740	3273	2050	39694	45366	28585	30918	20541	17382	11149	7000
1985	5756	5670	4409	3980	3270	2860	3360	3270	22140	21315	17544	14186	12186	8462	8218	8258
1986	6284	7650	4550	5070	3434	3010	2756	2570	26063	35274	19776	22708	11990	11333	8144	7891
1987	6180	4710	5014	3820	3401	2520	2725	2460	22852	18584	17639	14776	9903	8680	7347	7414
1988	3175	2130	2972	1480	2406	1540	3427	1530	10378	4674	9845	2525	7629	2524	6431	2164
1989	6758	8310	5372	8520	3579	3560	3340	3960	19207	17314	15313	17902	8453	5270	6770	5147
1990	10735	13500	8260	6890	4724	4310	2673	3690	34861	36813	24760	23264	12379	14335	8289	11185
1991	11184	9240	7418	4590	4849	2840	2874	2510	40243	35772	28265	18731	16010	10062	9599	8104
1992	3628	4920	3084	4780	2568	5900	2587	3500	12358	14835	11260	14967	8974	19610	6980	10322
1993	9887	9120	5878	8220	4490	9690	3639	6560	46759	40591	32790	40674	22914	52641	11934	30940
1994	6458	5220	4147	4740	3489	3480	3436	2810	22887	17737	18342	18275	15049	11522	9259	7145
1995	12495	13300	8971	7610	5202	4750	3146	2960	44192	49676	29920	32104	12878	17483	8474	6990
1996	9797	11700	6038	5810	4463	4790	3692	3290	36749	47578	26113	23262	14439	18030	9041	8291
1997	7001	9140	5553	6520	3653	3530	3401	2770	24710	33762	19058	25115	12393	10400	8294	6250
1998	6777	7330	4941	8150	3586	4760	2902	2730	29851	34567	22752	41918	18203	21440	10359	7807
1999	8043	6930	6262	6220	3961	3430	2829	2150	36152	35830	26154	34465	17061	14497	9966	5503
2000	5037	5080	4519	5980	3040	3090	2705	2220	18331	21279	14899	26722	9148	10907	7049	5731
2001	6556	8080	5494	4720	3517	3370	3269	2690	24009	35089	18391	19025	10516	10963	7585	6419
2002	8433	9680	5380	3940	4075	2870	3128	2700	30172	34742	22416	14215	14220	8057	8962	5683
2003	8552	8800	5918	5370	4108	4260	3272	3760	29374	30068	21590	19023	11594	12916	7996	8610
2004	8394	9440	6616	7750	4062	3870	3053	4090	30481	34348	22212	28843	11611	12758	8002	11012
2005	4412	4400	4324	3540	2835	2270	2904	2940	17836	20465	14783	15242	10458	5964	7563	8525
2006	4285	3650	3887	2770	2793	2140	2601	2270	19677	17509	16116	11569	12328	6941	8270	6518
2007	7123	4880	5863	5830	3689	3620	3205	3530	27414	17792	20574	18662	12206	9270	8225	7238
2008	11507	9760	7449	8550	4937	5010	3460	5560	42257	34315	29513	27353	17005	15002	9946	13849
2009	9380	11200	5754	5670	4347	4800	3232	3910	33557	32794	24497	18261	15529	13244	9429	9351
2010	9360	8380	6209	7240	4339	5640	3325	3940	36202	29711	25764	22795	14119	15261	8926	9224
2011	14625	12700	8231	7390	5770	4610	3474	3670	55333	48184	37284	32661	21790	18430	11565	12412
2012	4256	2790	4230	2130	2783	1800	2303	1870	15399	10608	13139	8026	9070	6259	7018	5664
2013	10871	9810	7915	7710	4762	4550	3486	2730	44454	40902	30744	33015	17231	16925	10024	7293
2014	6012	7090	4552	6010	3350	3550	3821	3940	23275	29576	18193	25791	12111	12324	8189	11632
2015	13207	10500	9104	12700	5393	8150	3180	2820	42856	30497	28995	33812	11672	20916	8025	5934
2016	7966	7280	6164	4790	3939	5070	2682	4280	25352	21761	19241	17377	11080	18220	7801	13529

Table S3.2: Predicted by the regressions (pre) and observed (obs) monthly Mississippi River discharge and nitrogen loading

Year	Mississippi River															
	Discharge (m^3/s)								Loading (t/mo)							
	Jun		Jul		Aug		Sep		Jun		Jul		Aug		Sep	
	pre	obs	pre	obs	pre	obs	pre	obs	pre	obs	pre	obs	pre	obs	pre	obs
1980	14630	13600	11343	9490	8135	7860	8274	8010	63302	65152	47753	41706	26594	28307	20013	31300
1981	17920	20600	14115	14900	9121	11400	6541	8170	85438	101948	64589	84155	32983	62810	25417	34298
1982	19984	20400	15303	14600	9725	9990	9036	9200	111437	143000	81310	92394	41684	53563	26813	42533
1983	30025	34300	18650	14300	12537	8250	7422	6450	158722	139385	108588	78336	58501	34090	25718	20451
1984	20899	23300	13811	14000	10012	8710	7839	6850	98964	123543	69521	92867	39435	34138	20464	19808
1985	13430	13100	10561	9260	7762	7550	8034	7330	63122	57531	46965	32609	26875	19074	18873	16327
1986	14582	17700	11759	11800	8115	7530	6669	6360	80192	112690	59026	63614	32276	28958	21600	16855
1987	14336	10900	11802	9360	8037	5870	6600	5690	69577	55102	52856	34909	28267	14390	22124	13905
1988	7504	4990	7294	3600	5765	3790	8186	3720	28529	13023	23687	5649	14430	5606	15706	4847
1989	15744	19200	12198	19900	8475	8400	7990	9310	60823	60366	47098	48845	25237	15385	21538	19664
1990	25018	31400	17121	16000	11160	10100	6481	8560	123552	152546	88420	107462	45988	50702	26560	34340
1991	26414	20800	17243	10500	11552	6670	6937	6260	137626	126306	95863	58028	51343	24382	25282	16435
1992	8525	11500	7723	11200	6133	13700	6285	8200	45027	45566	34027	48241	20980	73102	15673	27006
1993	22938	21400	14949	19300	10591	22600	8664	15300	115379	112194	80188	118201	44809	129349	21813	83362
1994	15222	12100	10543	11000	8331	8130	8206	6550	52488	42928	39023	37795	23629	20355	16420	12330
1995	28816	31100	19949	17700	12190	11200	7552	6980	148559	119520	106812	73396	52928	39035	31448	16402
1996	22845	27800	15901	13800	10553	11200	8783	7580	108282	120410	78280	71102	41135	49456	25121	20769
1997	16390	21300	12093	15200	8676	8270	8127	6530	71260	85186	52775	60286	29443	24918	20274	15357
1998	15885	17100	11094	19100	8532	11100	7001	6390	70789	81083	50718	95731	30188	45490	17465	14843
1999	18721	16100	13442	14600	9369	8040	6836	5000	106351	104707	74928	88893	41555	36572	21925	12957
2000	11823	11900	10204	14100	7240	7320	6555	5110	47522	57404	37897	78568	20730	26753	19944	12637
2001	15158	19200	12123	11000	8293	7870	7829	6270	85153	121619	62349	63865	33905	27439	22101	15801
2002	18892	23700	13398	9700	9421	6720	7512	6270	94489	102801	67602	40437	37445	17896	21548	16069
2003	19866	20500	14520	12500	9698	9950	7837	8770	85290	73729	63743	46583	33301	29705	24185	20424
2004	19567	22100	14597	18000	9609	9040	7342	9560	82223	105046	62274	82273	32006	32300	24860	31175
2005	10357	10300	9081	8310	6759	5320	7005	6700	44643	51898	35040	36541	20171	11757	17965	16424
2006	10063	8520	8742	6520	6662	5030	6318	5250	50570	45046	38259	24619	22678	14307	17130	14367
2007	16629	11400	12723	13600	8743	8500	7686	8240	96467	58336	69220	47943	37933	24456	22192	26493
2008	26572	22900	17298	19800	11596	11900	8261	13000	134343	123993	93922	116997	50200	51038	25279	32924
2009	21873	25800	14647	13200	10286	11300	7747	9310	93845	99627	67573	59025	37033	32443	22081	25662
2010	21729	19500	15505	16900	10234	13100	7955	9400	94532	85273	70005	79933	36271	52511	25184	26967
2011	33637	29400	20297	17300	13498	11300	8291	8640	130702	126513	92985	88569	48326	48527	26979	28920
2012	9983	6480	8905	5010	6633	4270	5641	4470	38066	22103	30847	14271	17656	10947	17884	10418
2013	25395	23000	17154	17800	11267	10700	8318	6520	133928	120485	94353	85009	49718	39466	26209	17208
2014	14058	16500	11030	14200	7957	8340	9071	9140	61880	75217	46687	71543	26166	31228	19685	32470
2015	29842	22800	20601	29000	12465	18400	7629	7450	138028	116387	101115	130076	49036	71268	32390	24406
2016	17926	16200	13240	12300	9132	12400	6501	11100	87152	82778	63664	63570	34571	62689	22265	51302

S4 Forecast skill and variance assessment

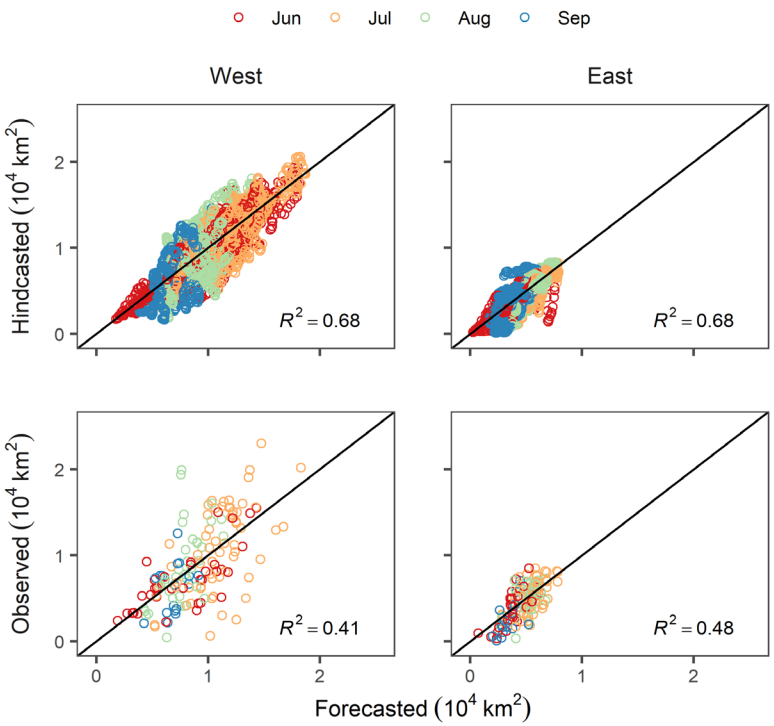

Figure S4.1: Daily hindcasted HA and observed HA versus pseudo-forecasted HA for the west and east sections. Diagonal line represents perfect prediction.

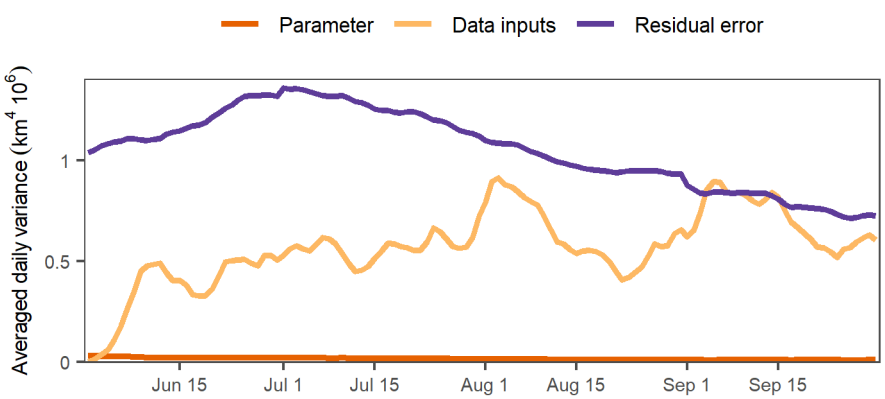

Figure S4.2: Averaged daily variance of total HA due to different sources of uncertainty. In this case, the "residual error" variance includes transformation and bias uncertainties, in addition to the DMO20 residuals. Note that the relative magnitudes of the variance components are somewhat different from the magnitudes of the IQR components (e.g., Fig. 5) because variance has squared units.

S5 HA pseudo-forecast for west and east sections of the shelf

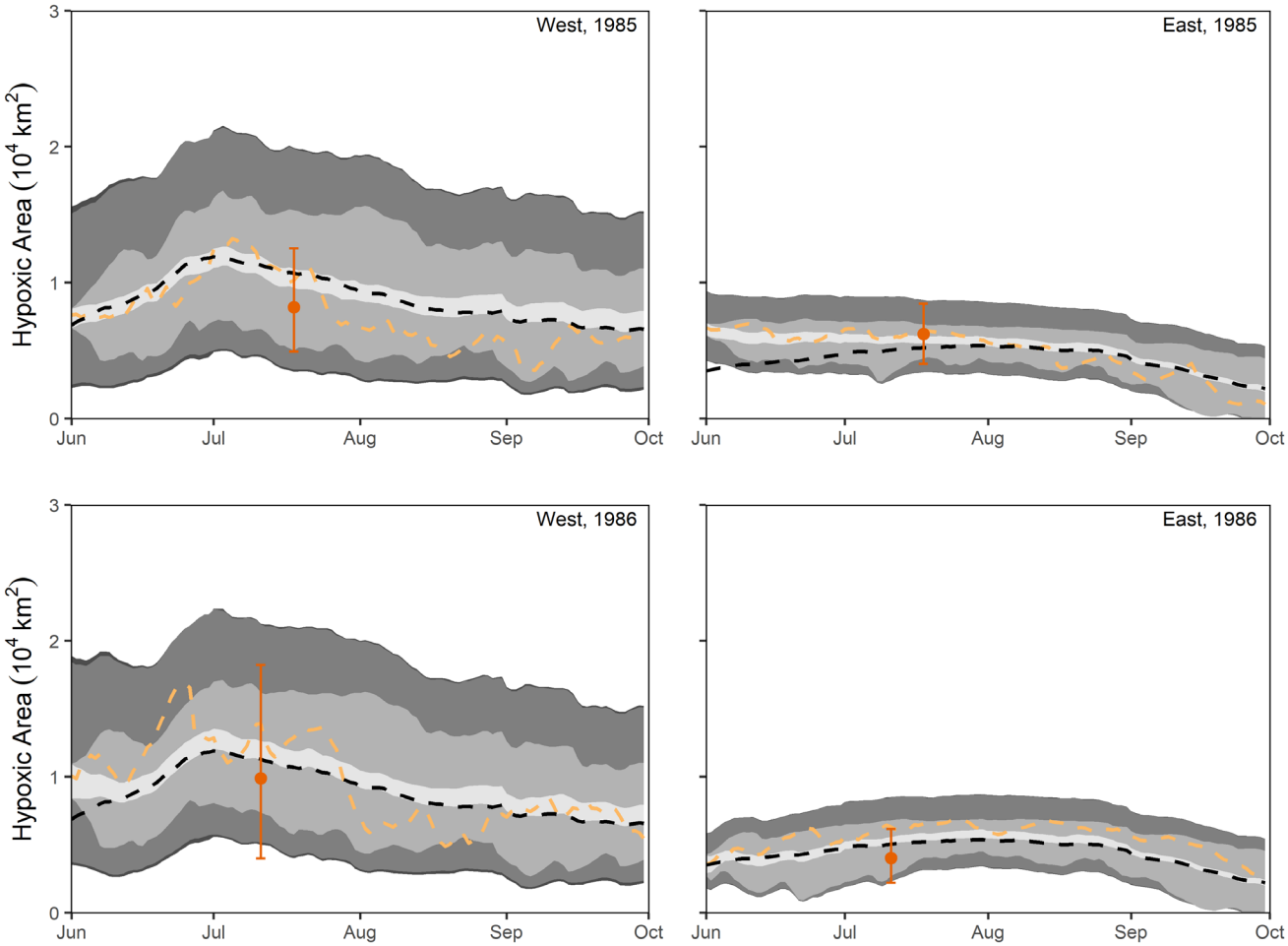

Figure S5.1: Daily pseudo-forecasts of HA for the west and east sections in 1985 (top) and 1986 (bottom), including 95% IQR of the predictive distribution, distinguishing between i) parameter, ii) hydrometeorological inputs, iii) mechanistic model error, and iv) regressions related to transformation of BWDO to HA and bias adjustment uncertainties (shades of gray from lightest to darkest). Yellow dashed line is hindcasted estimate, black dashed line is the 32-year average hindcast, orange points and error bars represent the mean and associated 95% confidence interval of the (geostatistically estimated) hypoxia observations.

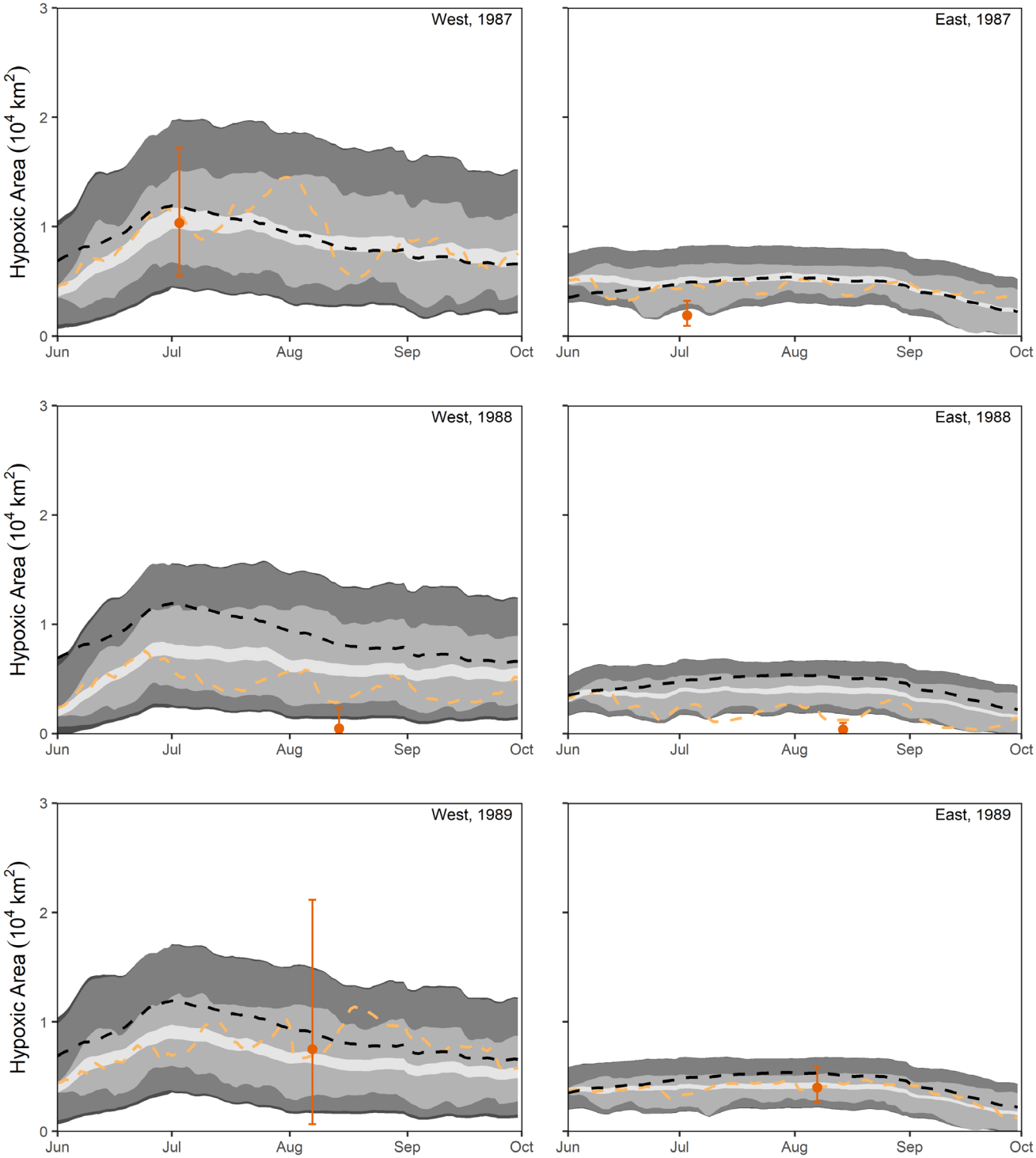

Figure S5.2: Pseudo-forecast as in Fig. S5.1 but for different years.

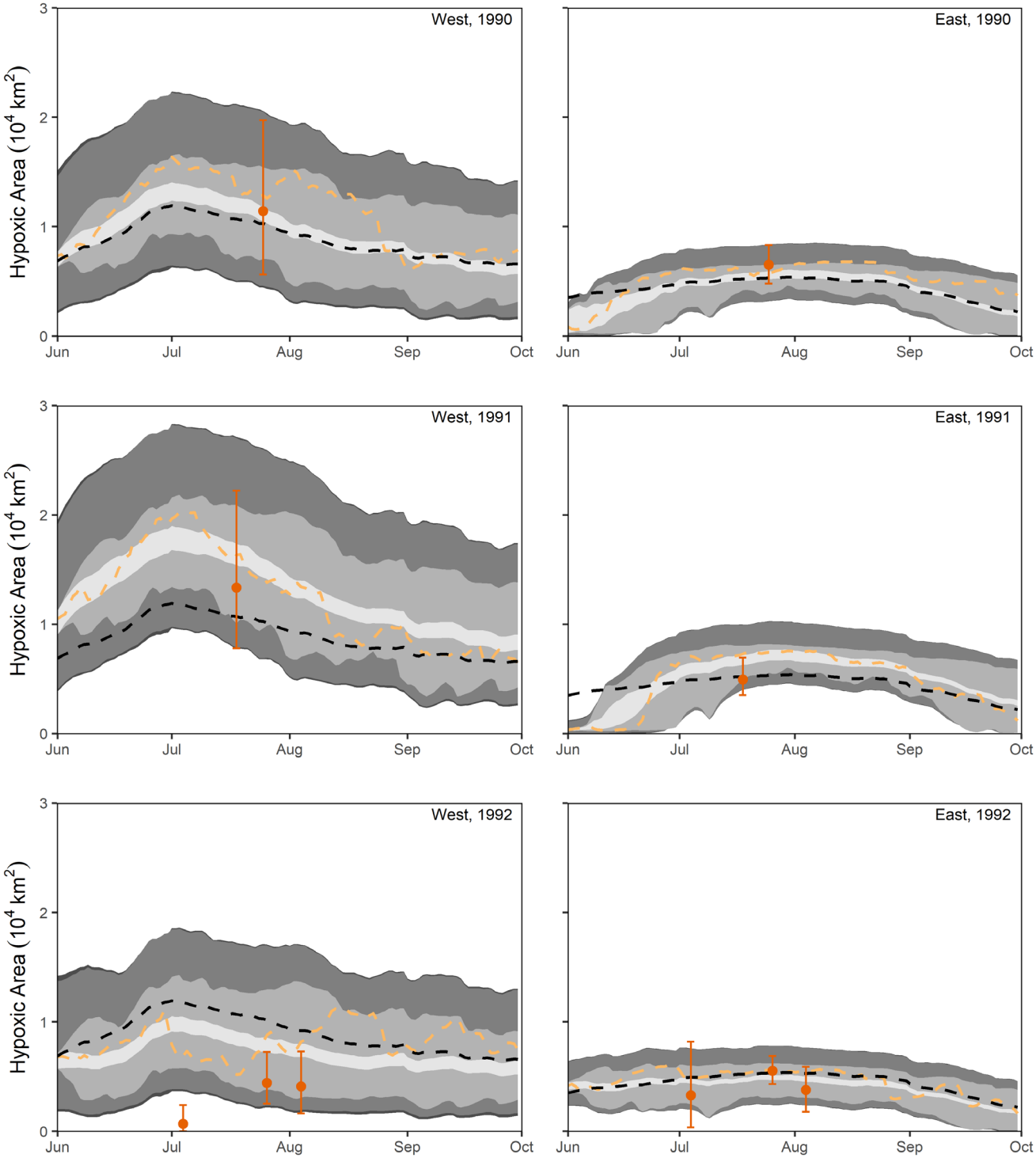

Figure S5.3: Pseudo-forecast as in Fig. S5.1 but for different years.

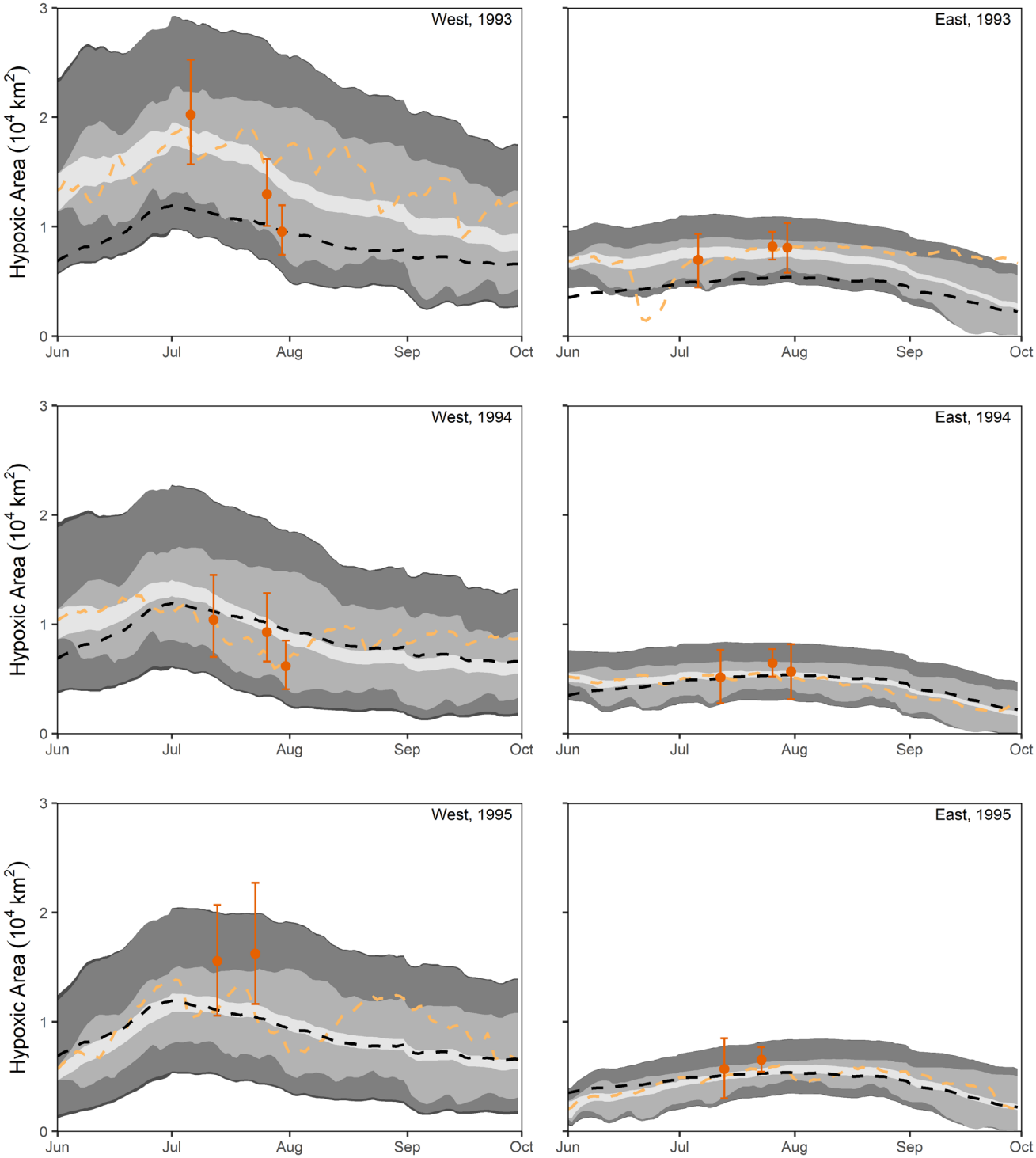

Figure S5.4: Pseudo-forecast as in Fig. S5.1 but for different years.

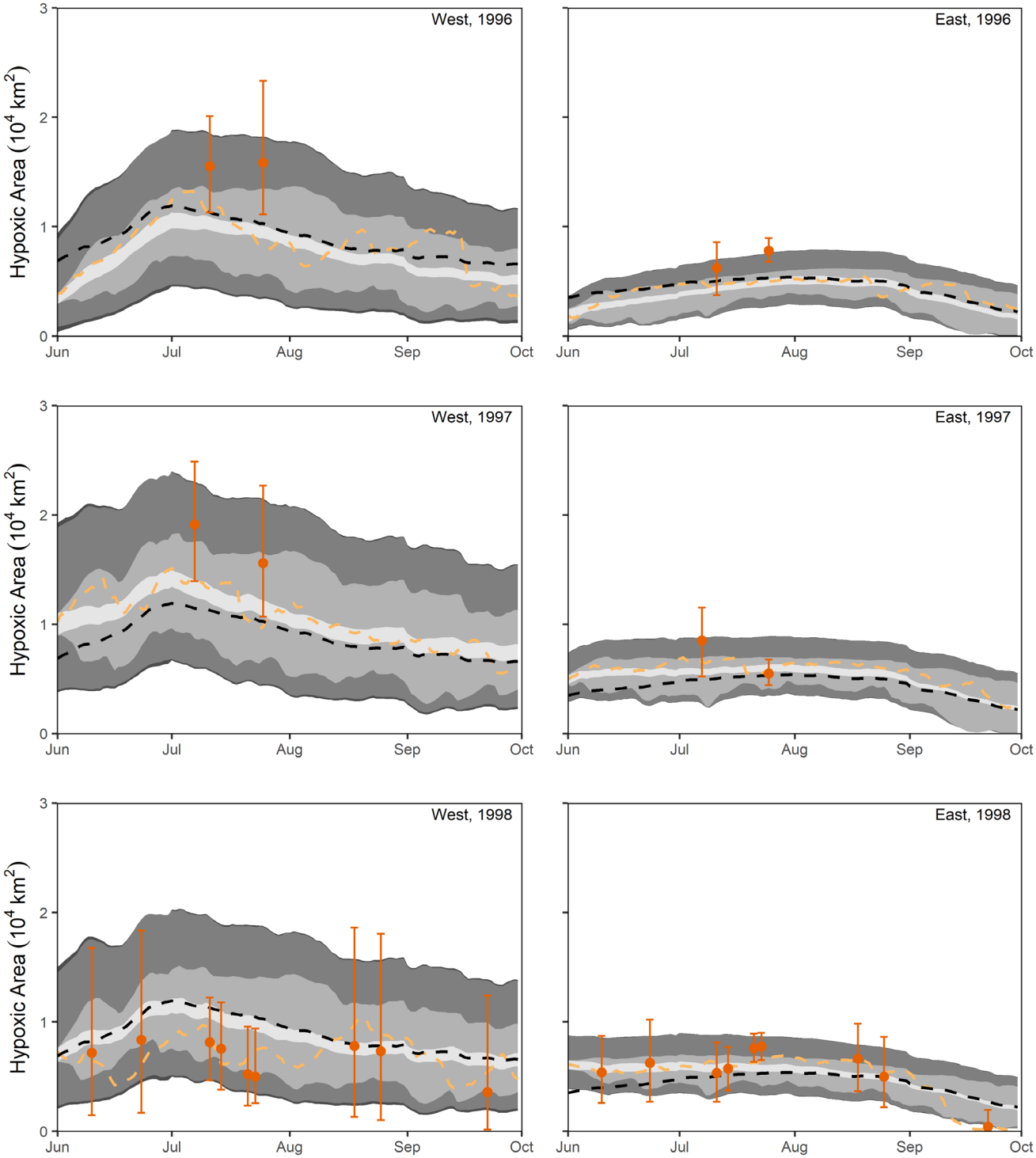

Figure S5.5: Pseudo-forecast as in Fig. S5.1 but for different years.

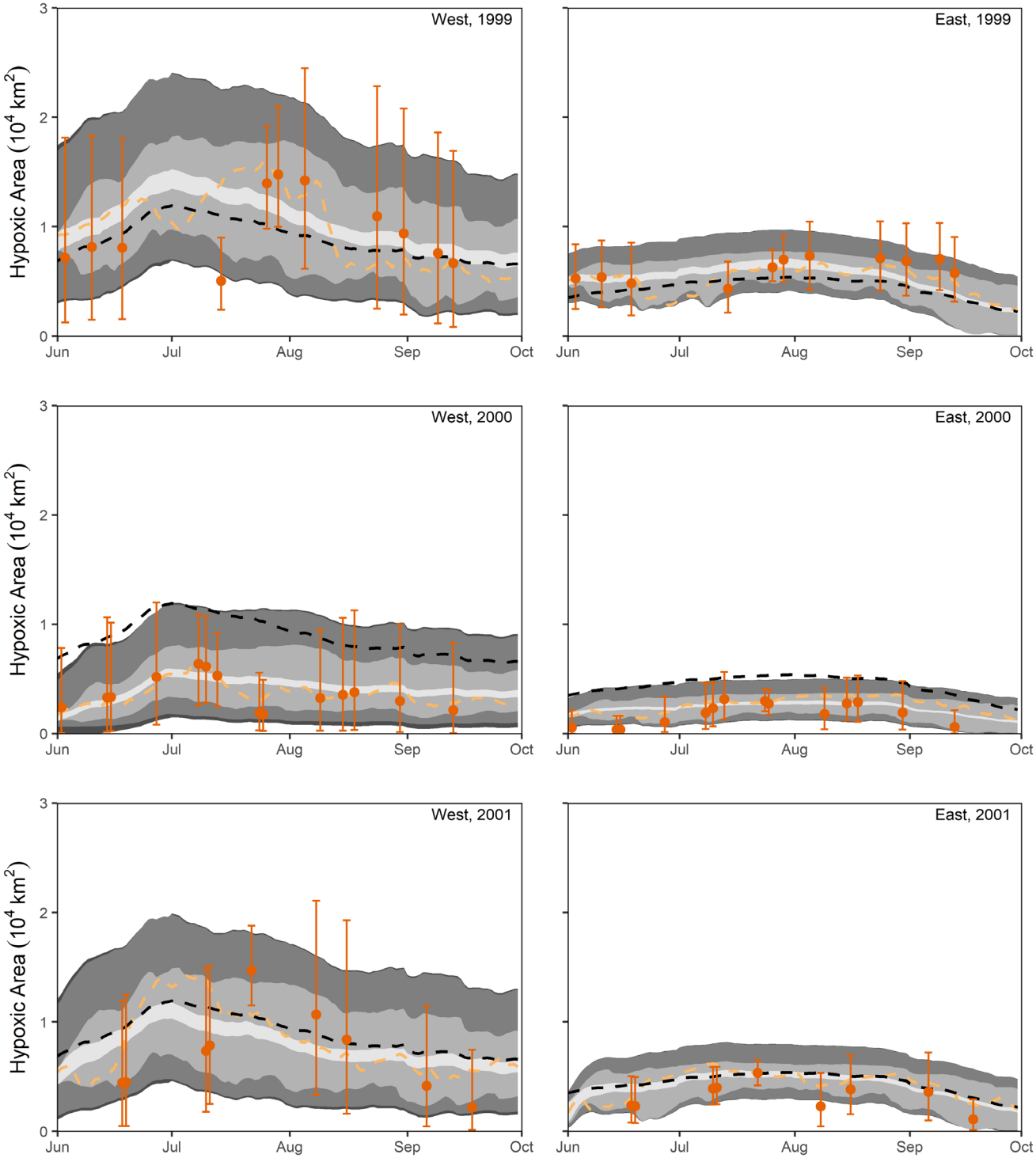

Figure S5.6: Pseudo-forecast as in Fig. S5.1 but for different years.

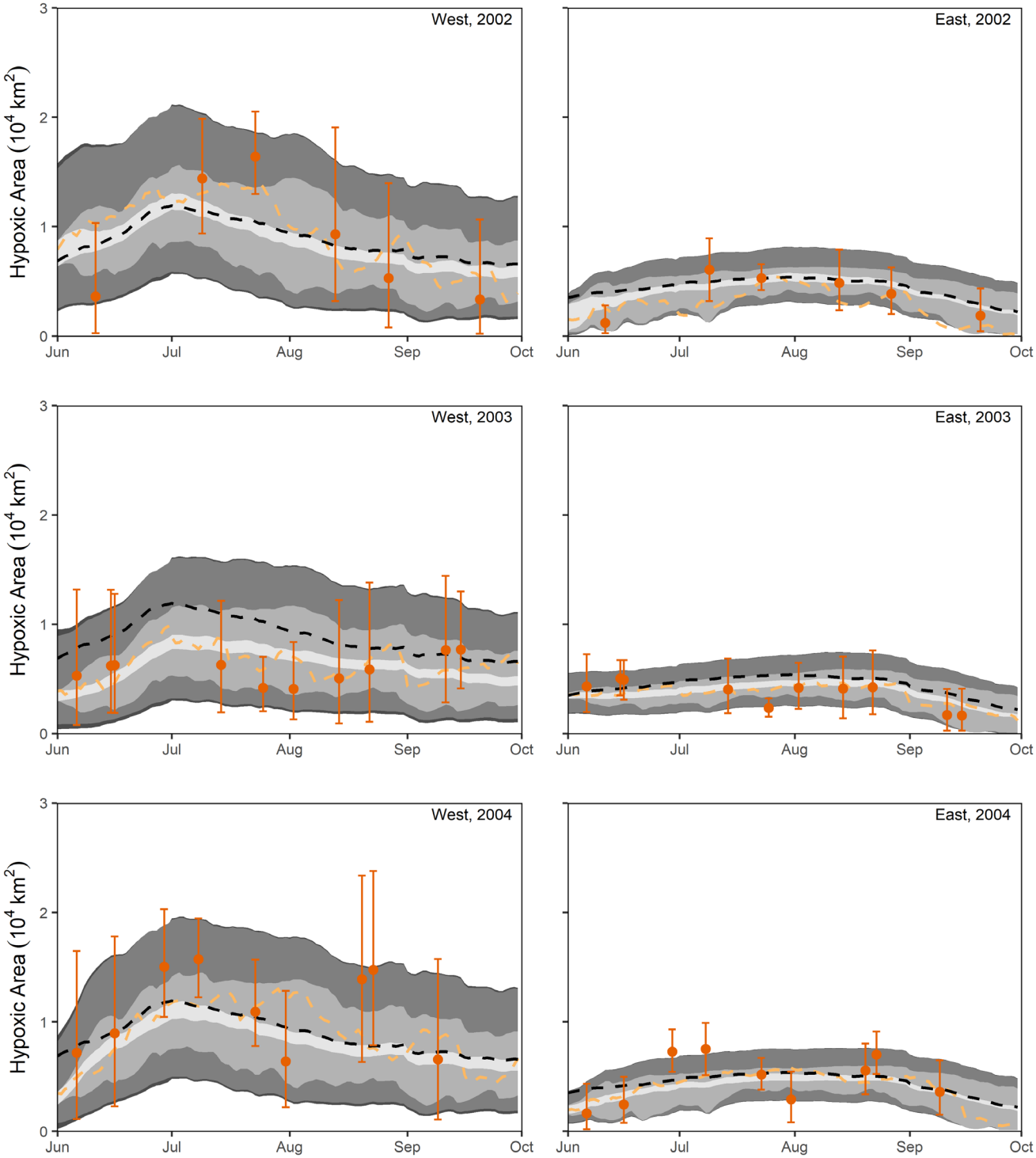

Figure S5.7: Pseudo-forecast as in Fig. S5.1 but for different years.

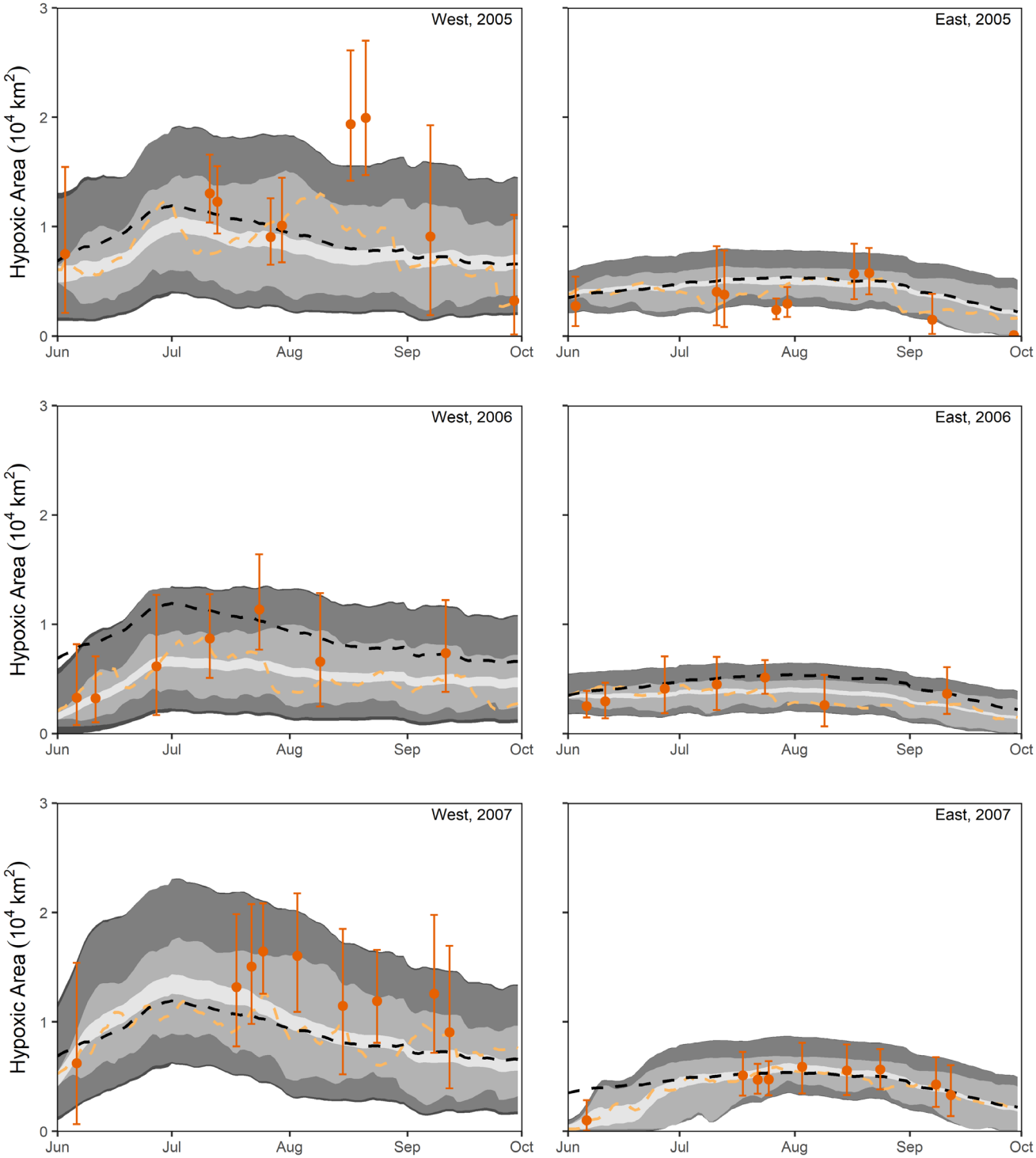

Figure S5.8: Pseudo-forecast as in Fig. S5.1 but for different years.

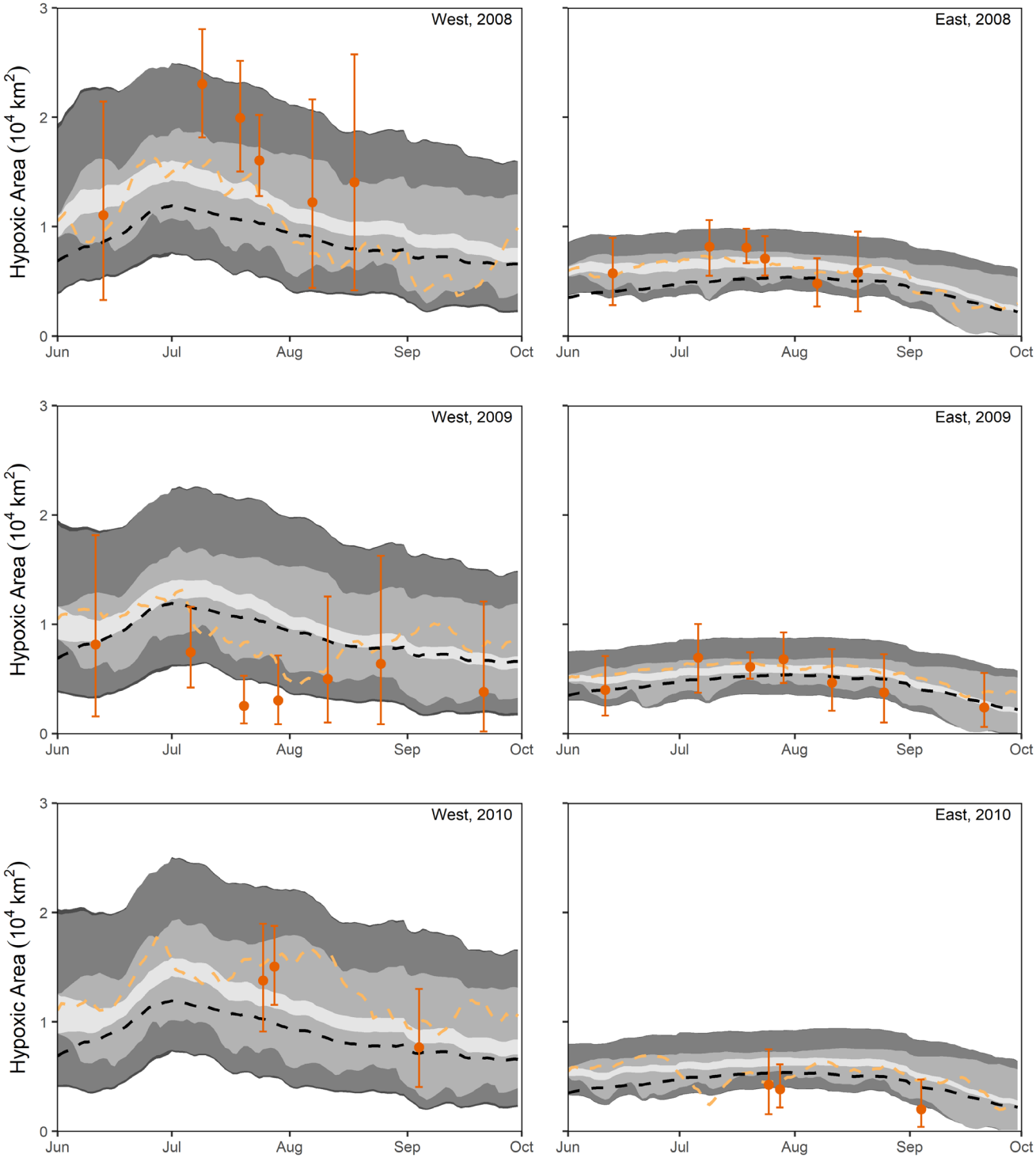

Figure S5.9: Pseudo-forecast as in Fig. S5.1 but for different years.

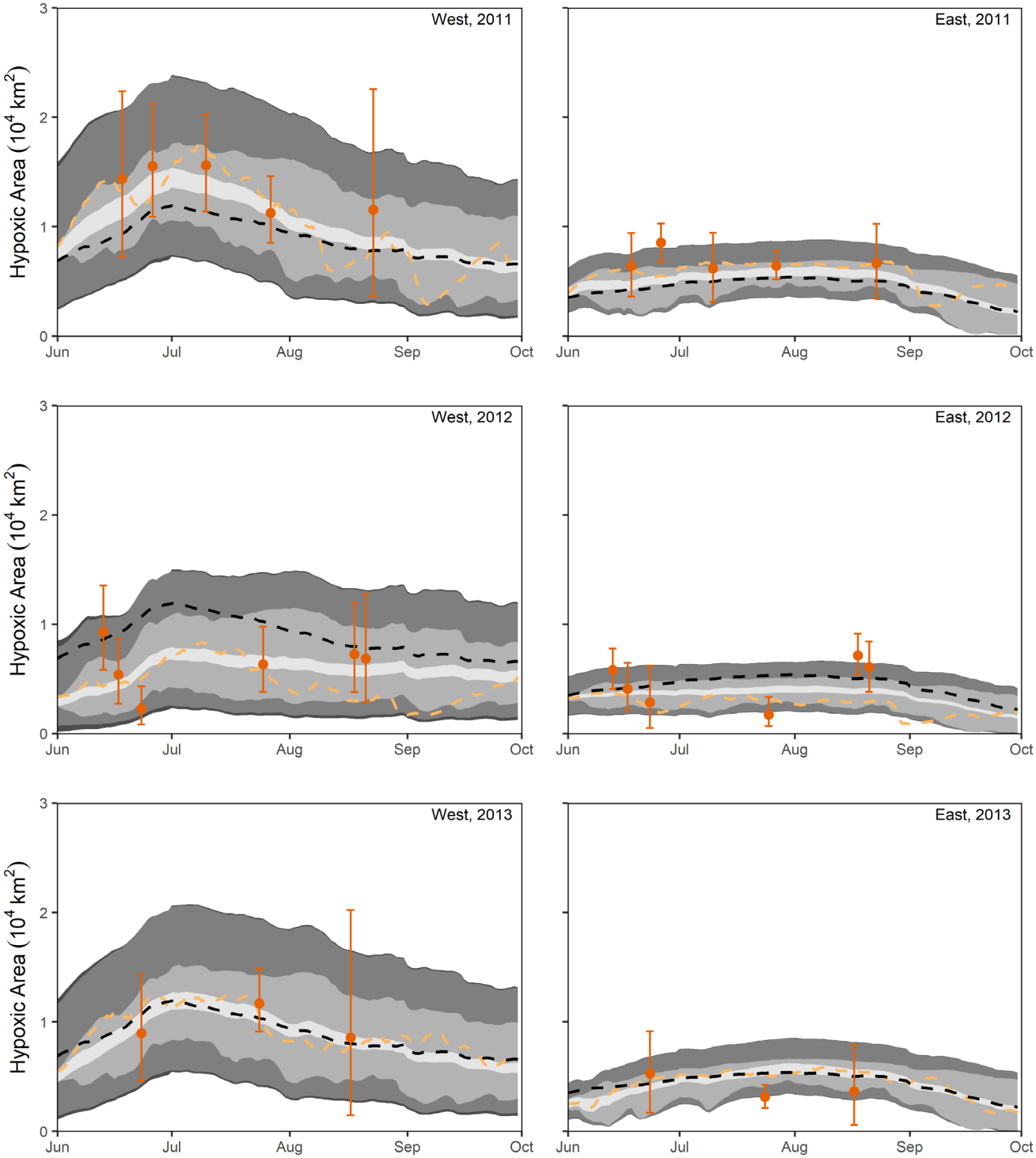

Figure S5.10: Pseudo-forecast as in Fig. S5.1 but for different years.

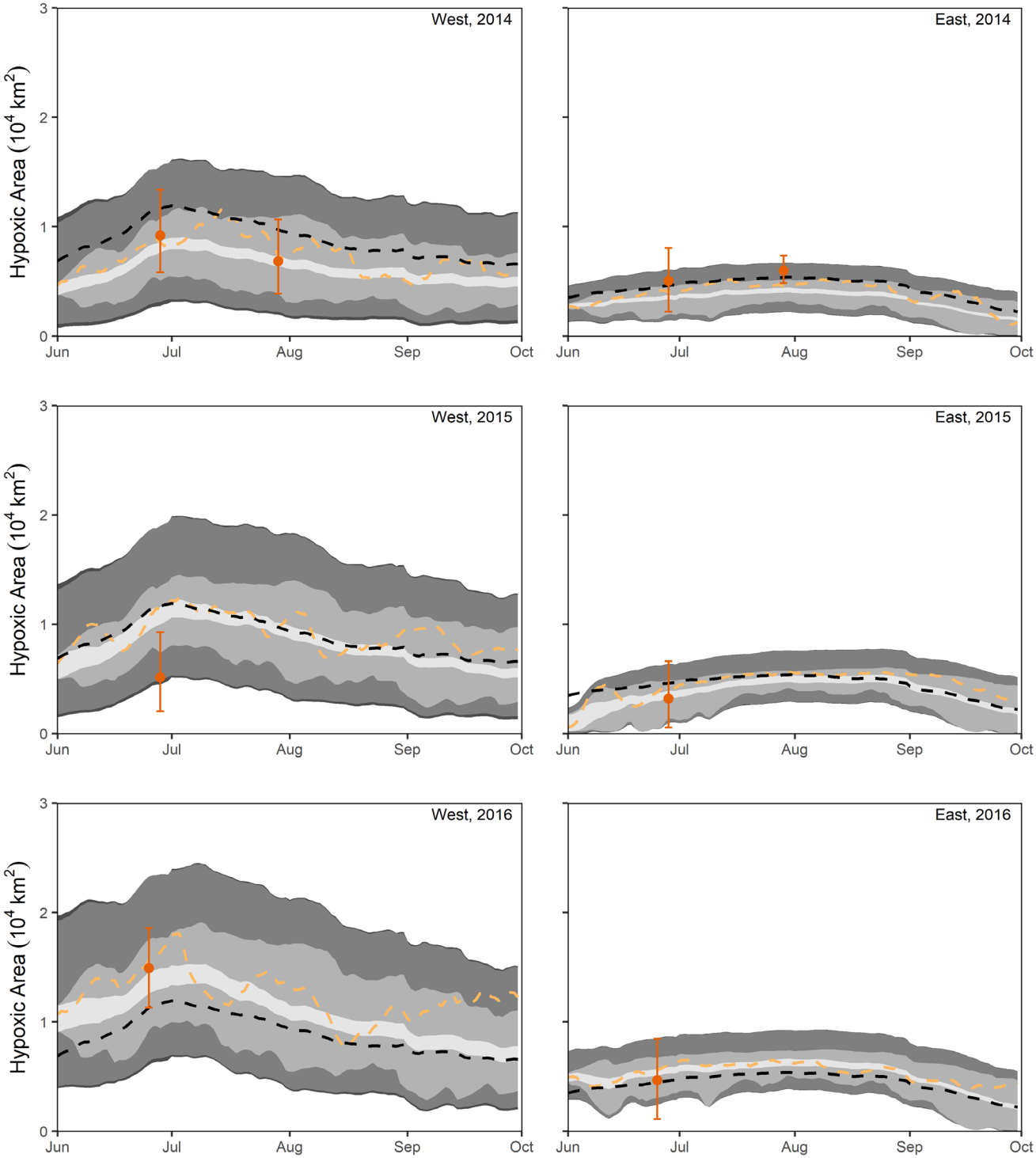

Figure S5.11: Pseudo-forecast as in Fig. S5.1 but for different years.

S6 Total HA pseudo-forecast

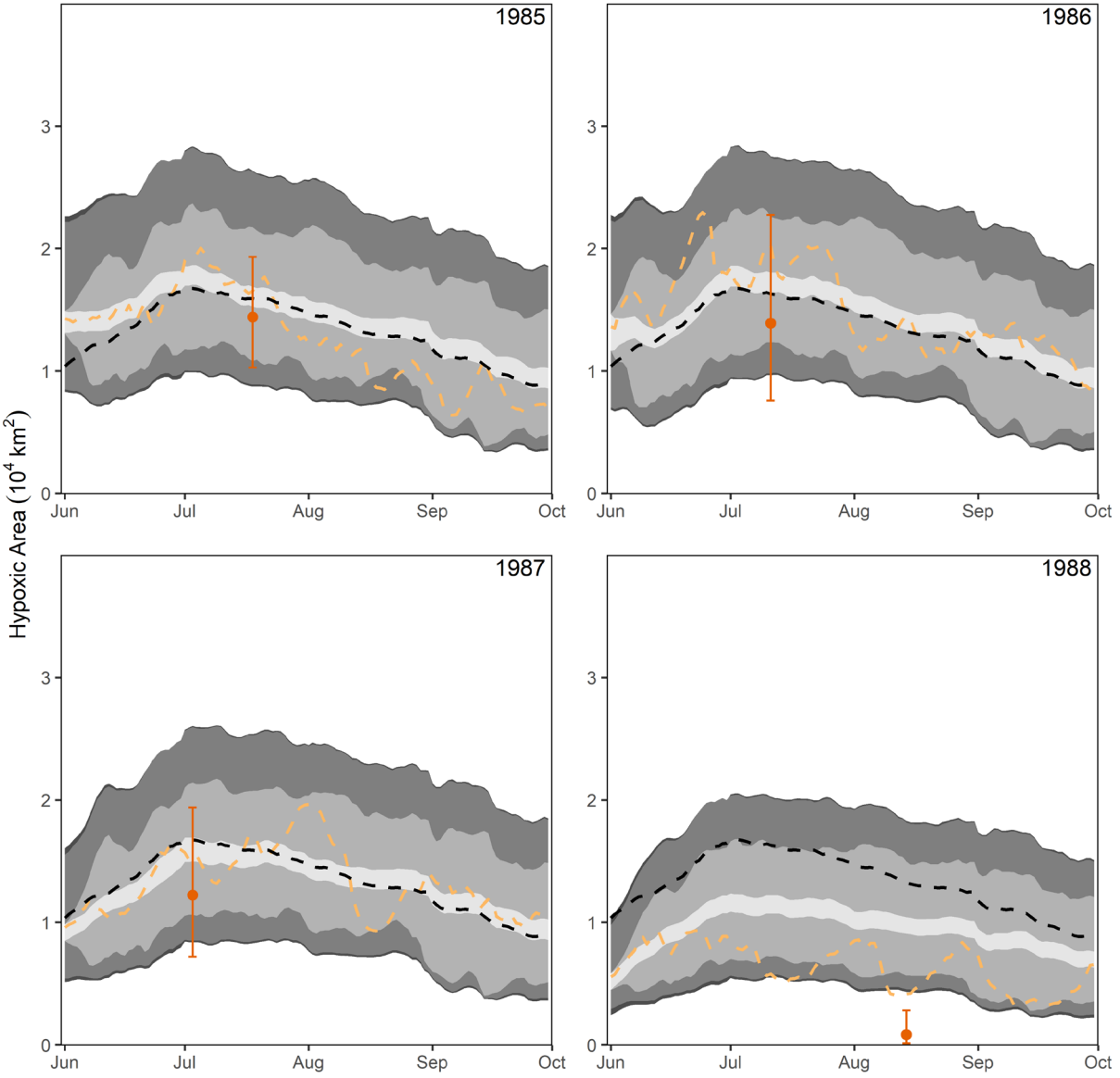

Figure S6.1: Daily pseudo-forecasts of total HA, including 95% IQR of the predictive distribution (1985-1988), distinguishing between i) parameter, ii) hydrometeorological inputs, iii) mechanistic model error and iv) regressions related to transformation of BWDO to HA and bias adjustment uncertainties (shades of gray from lightest to darkest). Yellow dashed line is hindcasted estimate, black dashed line is the 32-year average hindcast, orange points and error bars represent the mean and associated 95% confidence interval of the (geostatistically estimated) hypoxia observations.

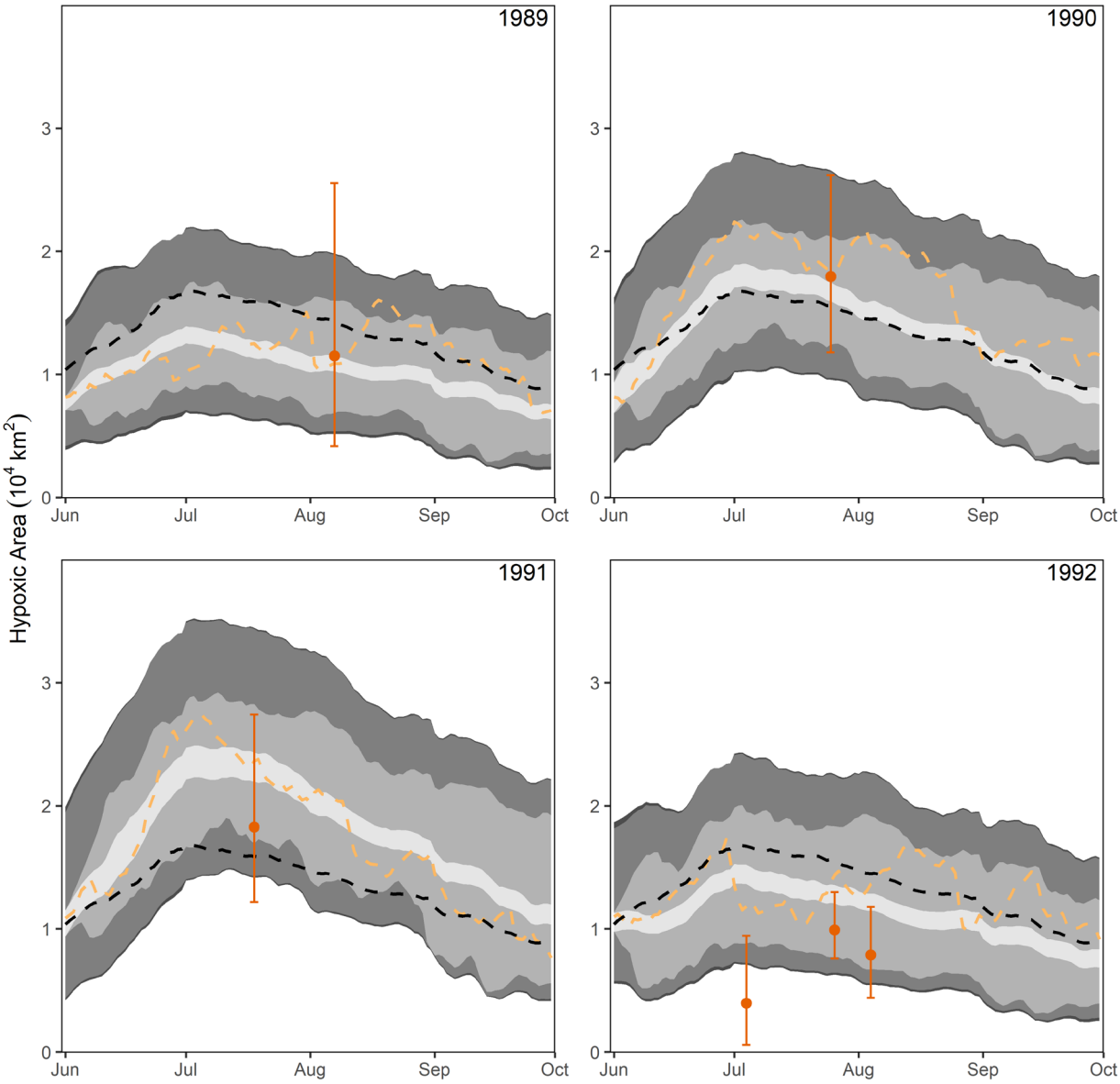

Figure S6.2: Pseudo-forecast as in Fig. S6.1 but for different years.

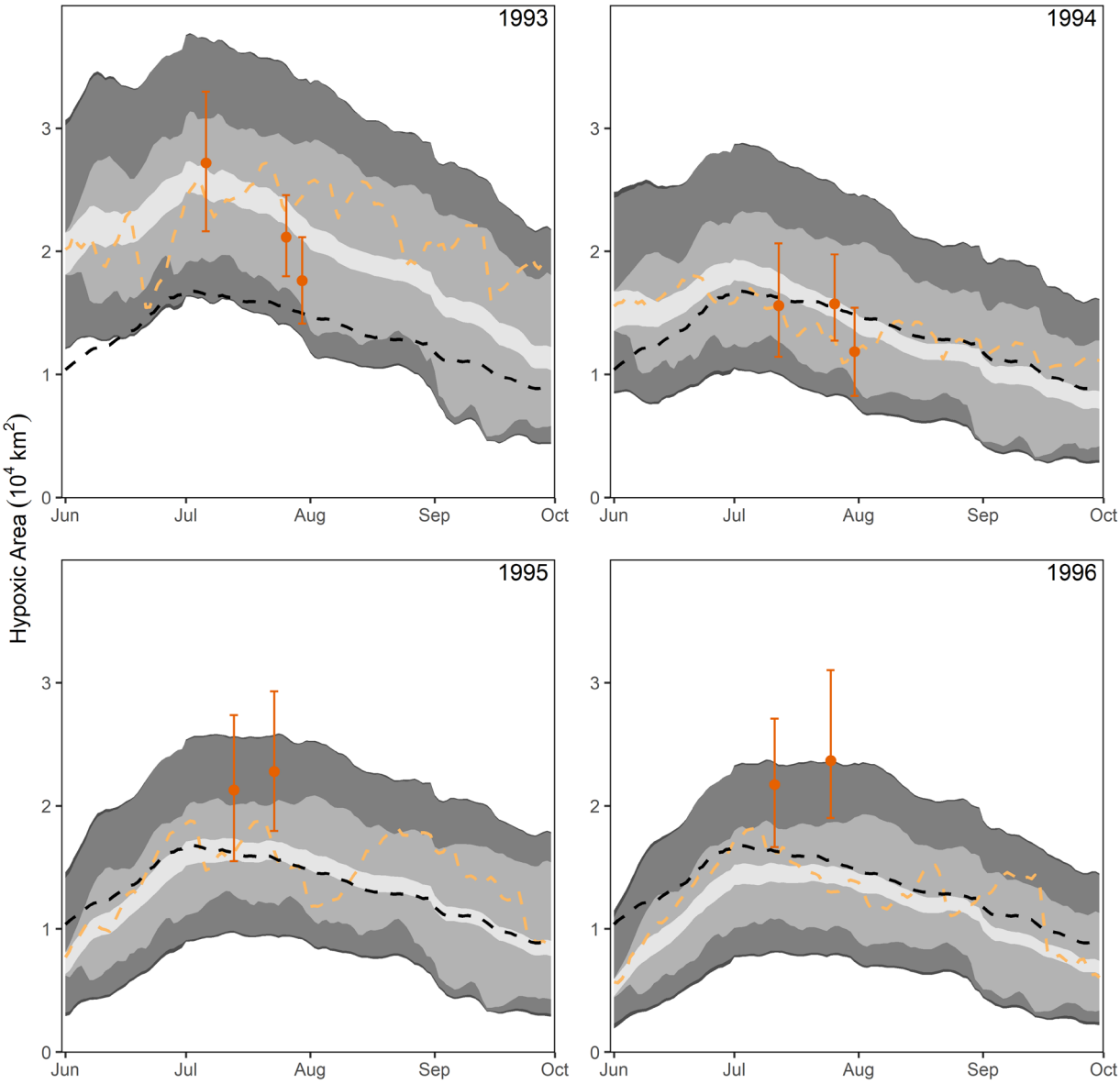

Figure S6.3: Pseudo-forecast as in Fig. S6.1 but for different years.

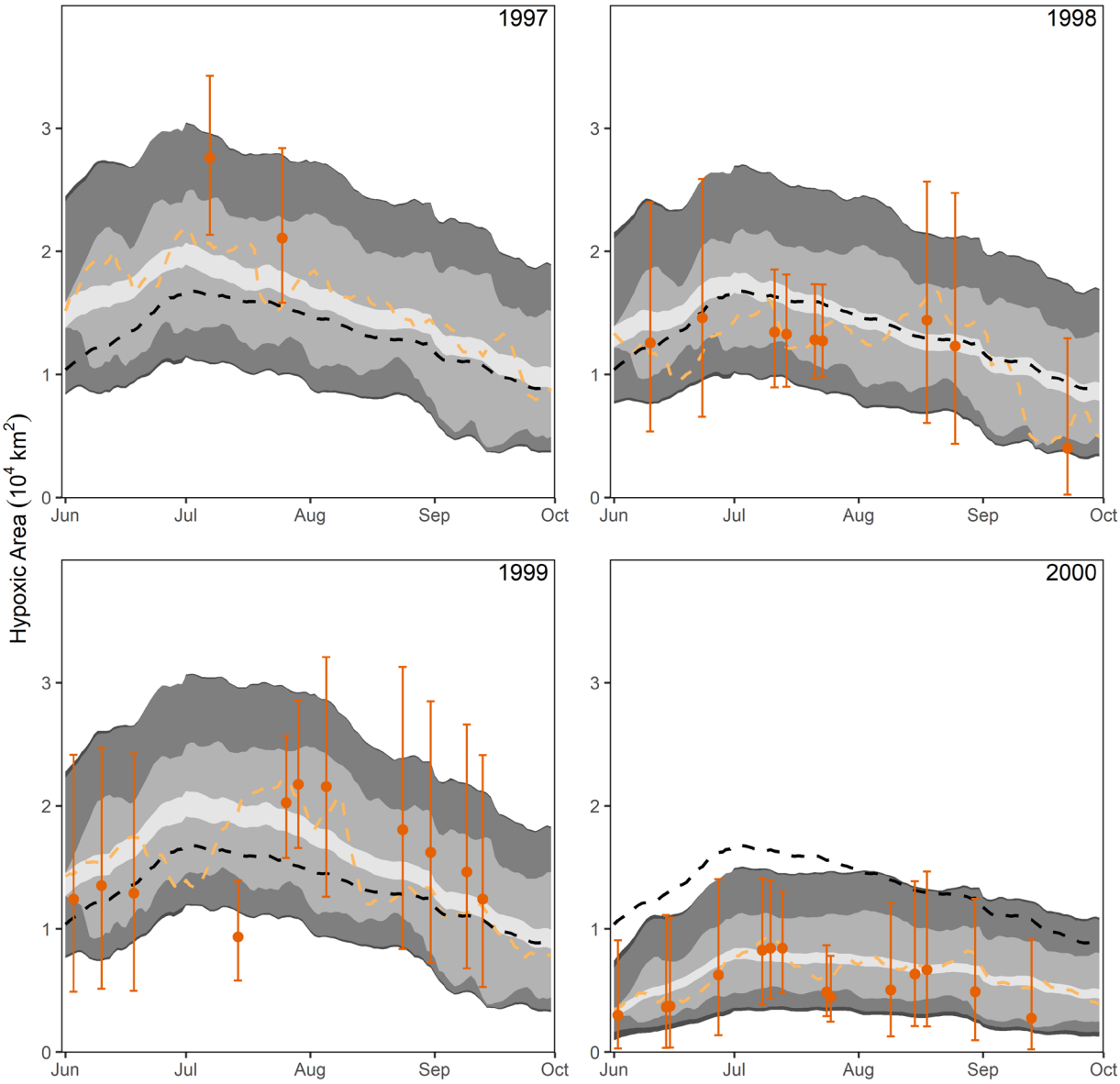

Figure S6.4: Pseudo-forecast as in Fig. S6.1 but for different years.

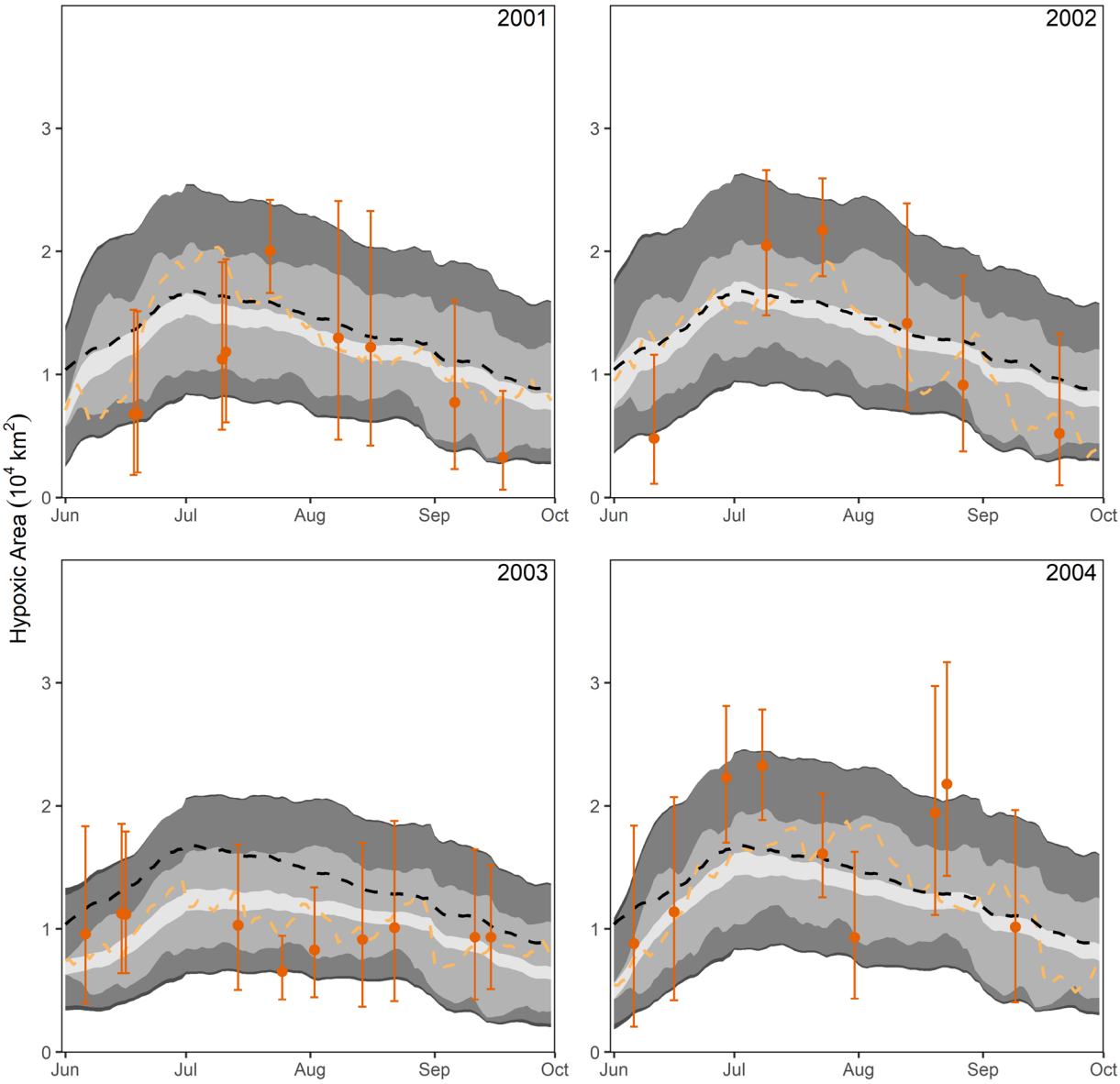

Figure S6.5: Pseudo-forecast as in Fig. S6.1 but for different years.

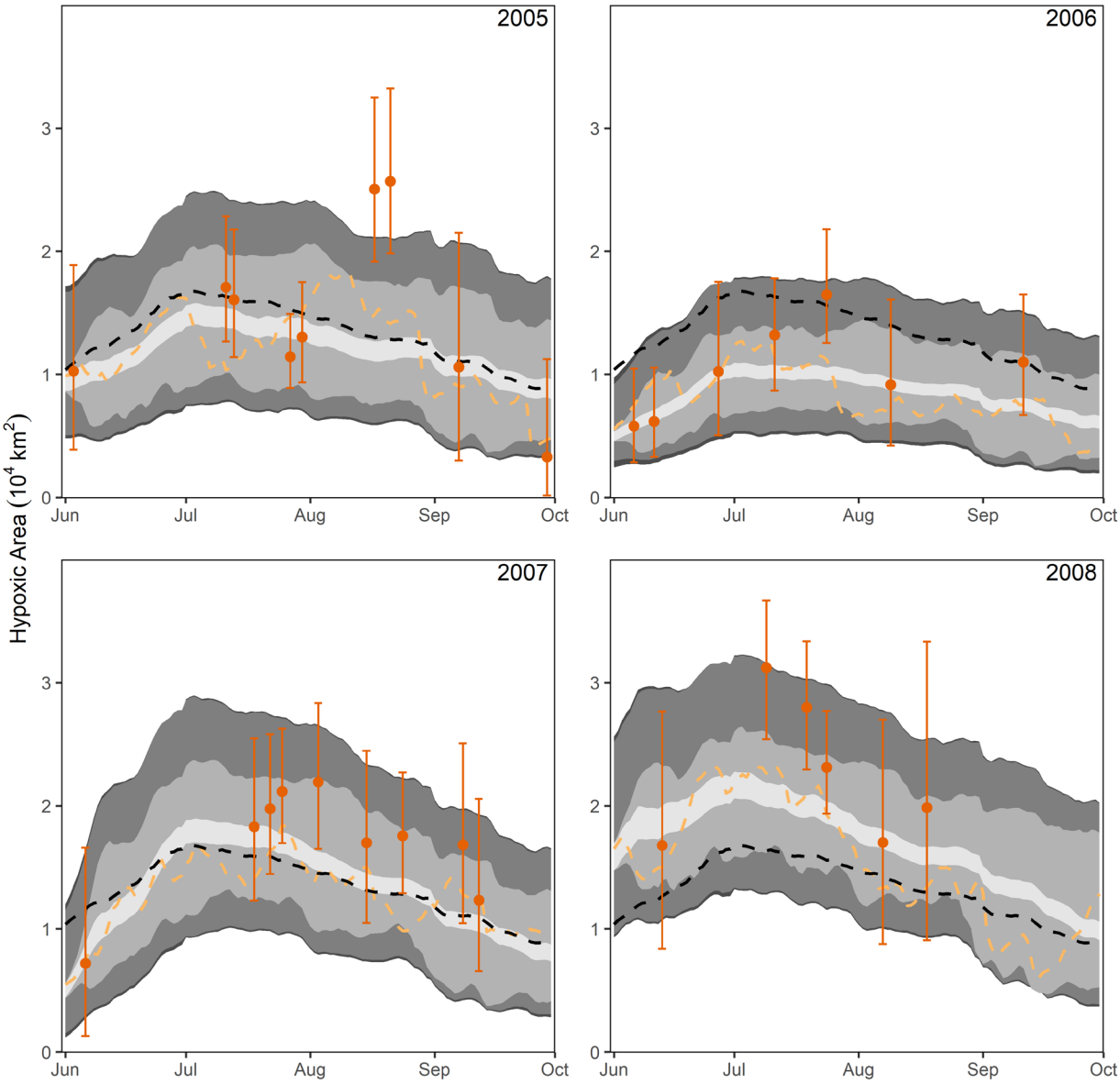

Figure S6.6: Pseudo-forecast as in Fig. S6.1 but for different years.

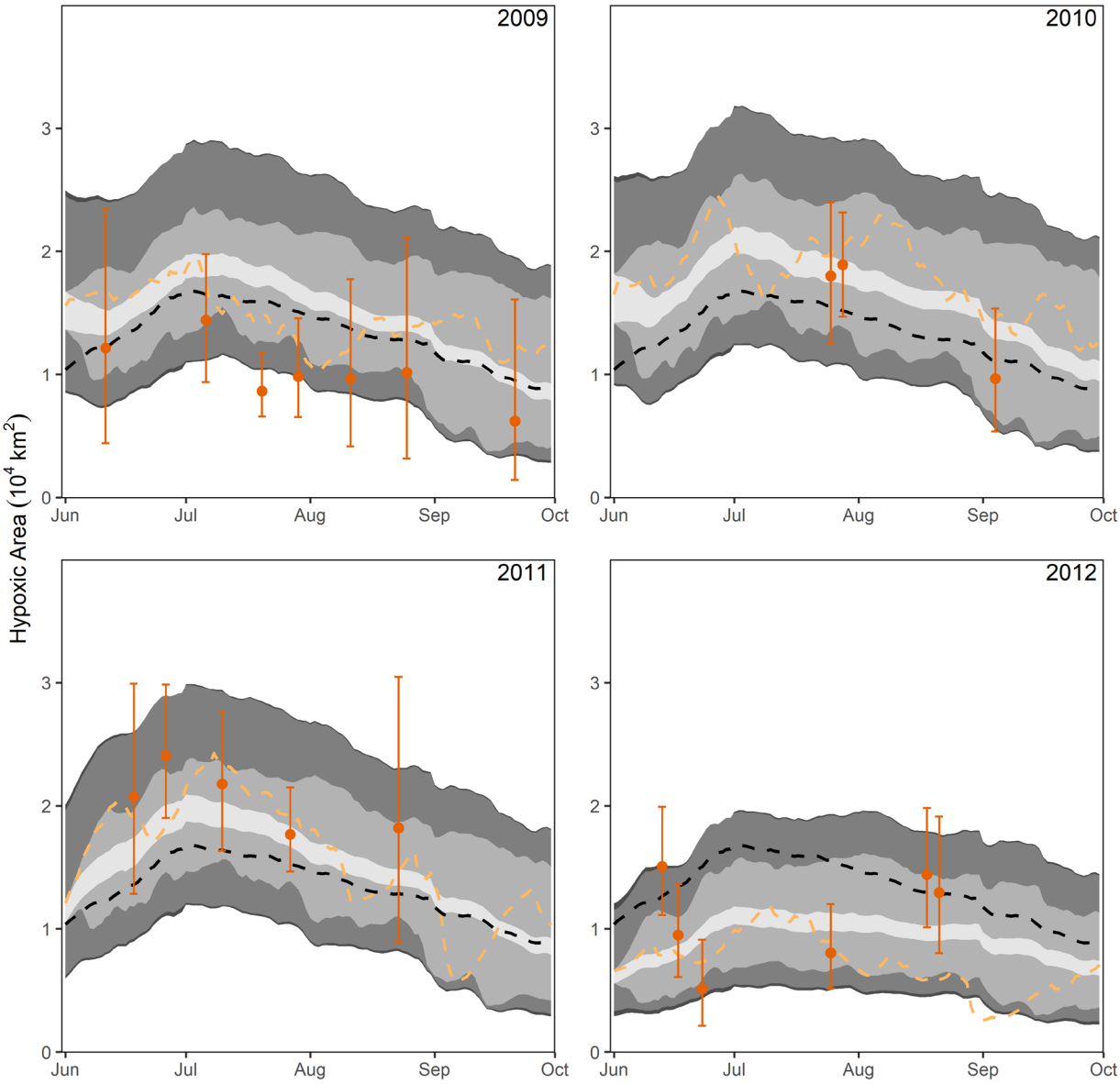

Figure S6.7: Pseudo-forecast as in Fig. S6.1 but for different years.

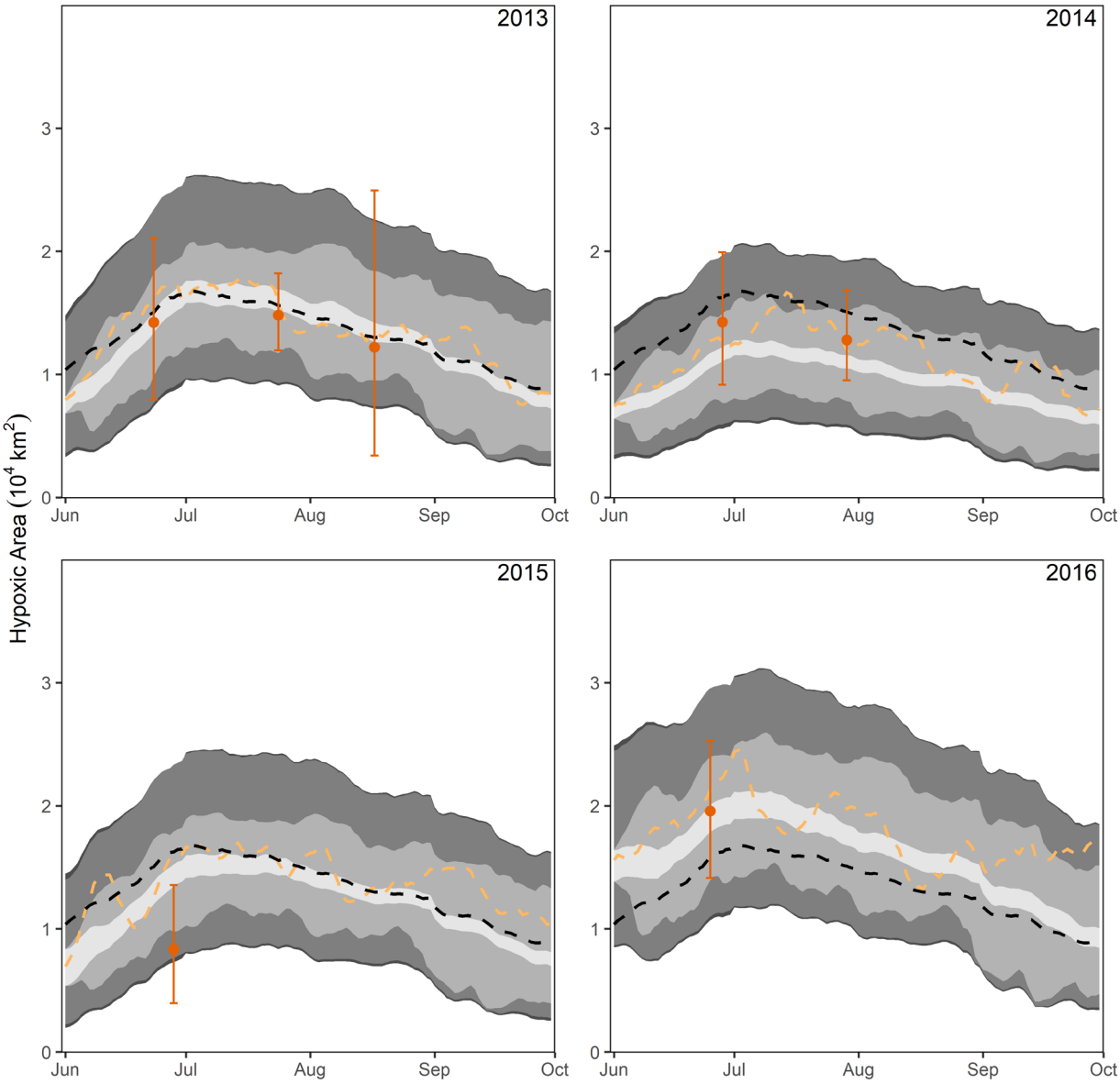

Figure S6.8: Pseudo-forecast as in Fig. S6.1 but for different years.

References

Del Giudice, D., Matli, V. R. R. and Obenour, D. R.: Bayesian mechanistic modeling characterizes Gulf of Mexico hypoxia: 1968–2016 and future scenarios, Ecol. Appl., 30(2), eap.2032, doi:10.1002/eap.2032, 2020.

Obenour, D. R., Michalak, A. M. and Scavia, D.: Assessing biophysical controls on Gulf of Mexico hypoxia through probabilistic modeling, Ecol. Appl., 25(2), 492–505, doi:10.1890/13-2257.1, 2015.